monoclonal; Chemicon), galactocerebroside (GalC, 1:200, monoclonal; Chemicon), and glial fibrillary acidic protein (GFAP, 1:1,000, polyclonal; DAKO, Carpinteria, CA) for 1 hr at room temperature. For 5-bromo-2′-deoxyuridine (BrdU) staining, the cells were incubated in 10 nM BrdU for 1 hr. Slides were fixed in methanol for 10 min at 4°C, permeabilized in 0.2% Triton X-100, and treated with 2 M HCl followed by 0.1 M NaB_2O_7 before immunostaining. Fluorophore-labeled secondary antibodies (Alexa Fluor 488 goat antimouse IgG [H+L] and Alexa Fluor 594 goat antimouse IgG [H+L]) were used for detection. Hoechst 33342 (1:5,000) was used (10 min at room temperature) for nuclear staining. Sections were viewed with a Nikon Eclipse E800 microscope at excitation wavelengths of 488 and 594 nm.

Binding Assay

Rat or human NPCs were plated in 48-well plates at 3×10^4 cells/well in NPMM. After 2 days in culture, cells were 70–80% confluent and were washed once with NPBM for rat NPCs and Ex Vivo 15 media for human NPCs. Competition binding assays were carried out at room temperatures in 250 μl of binding buffer (NPBM for rat or Ex Vivo 15 media for human NPCs plus 1% of BSA) containing 50 pM [^{125}I]-SDF-1α (1.5×10^5 cpm/ml, Amersham Biosciences, Piscataway, NJ) in the presence of an increasing concentration of unlabeled SDF-1α or T140 for 2 hr. After incubation, cells were washed three times with binding buffer and lysed with 1% Triton X-100 in PBS. Lysates were transferred to glass test tubes and counted in a γ counter.

Cyclic AMP Assay

The assay for cAMP accumulation was carried out as described previously with minor modifications (Zheng et al., 1999). Briefly, rat or human NPCs were plated at a density of 1×10^5 cells/well in 24-well plates coated with poly-D-lysine for 2 days. Cells were loaded with 5 μCi [^{3}H] adenine (Perkin-Elmer, Wellesley, MA) at 0.5 ml/well NPMM for 90–120 min at 37°C. For T140 and pertussis toxin (PTX) blocking, 10 nM T140 or 100 ng/ml PTX were added at 1 and 6 hr, respectively, before stimulation. Cells were then washed twice with fresh media and treated with 60 μM forskolin (FSK; Sigma) with and without different concentrations of SDF-1α, fractalkine, interferon γ-inducible protein 10 (IP-10) or interleukin 8 (IL-8). Intracellular [^{3}H] cAMP was extracted overnight with 1 ml of ice-cold 5% trichloroacetic acid (TCA) containing 1 mM unlabeled cAMP (internal control). [^{3}H] cAMP was separated from the titrated nucleotides by sequential ion-exchange chromatography over Dowex and Alumina columns (Sigma). The ATP and cAMP fractions (3 ml each) were collected in scintillation vials and 14 ml of Econo-Safe scintillation cocktail (Research Products International, Mt. Prospect, IL) was added. The radioactivity of samples was determined by liquid scintillation counting in a Packard scintillation counter (Perkin-Elmer Life and Analytical Sciences, Shelton, CT). Values are expressed as the percentage conversion of [^{3}H] ATP to [^{3}H] cAMP.

PI Hydrolysis Assay

Rat NPCs were plated at a density of 5×10^5 cells/dish in 25-mm Petri dishes coated with poly-D-lysine. After 2 days in culture, cells were labeled for 18–24 hr with 2 μCi [^{3}H] inositol (Amersham, Arlington Heights, IL) in 1 ml NPBM supplemented with NSF-1. For T140 and PTX blocking, 10 nM T140 and 100 ng/ml PTX were added at 1 and 6 hr before stimulation, respectively. After labeling, cells were washed and stimulated with different drugs in the presence of 10 mM LiCl. Labeled compounds were extracted from the cells with methanol and chloroform/water added as described elsewhere (Zheng et al., 1999). Labeled inositol phosphates were separated on Dowex 1-X8 (formate form; Sigma) columns and quantified by liquid scintillation counting.

Western Blot Assays

Rat or human NPCs were plated at 5×10^5 cells/well in 6-well poly-D-lysine-coated plates. Cells were treated with 100 ng/ml SDF-1α or 25 ng/ml bFGF for 1, 5, 10, or 30 min. For T140 and PTX blocking, 10 nM T140 and 100 ng/ml PTX were added at 30 min and 6 hr before SDF-1α stimulation, respectively. For Western blot analysis, proteins in cell culture homogenates were separated by 10% SDS-PAGE. After electrophoretic transfer to Immobilon-P membrane (polyvinylidene difluoride membranes; Millipore, Billerica, MA), proteins were treated with primary antibodies for phospho- or non-phosphoprotein kinases (extracellular signal-regulated kinases [ERK], Akt, and c-Jun N-terminal kinase [JNK], 1:1,000 dilution) (Cell Signaling Technologies, Beverly, MA) overnight at 4° C followed by a horseradish peroxidase-linked secondary anti-rabbit antibody (1:5,000 dilution; Cell Signaling Technologies). Antigen-antibody complexes were visualized by enhanced chemiluminescence Western blotting and captured with Hyperfilm ECL (Amersham). Gel and immunoblot images were quantitated using *NucleoVision* software (Nucleotech).

Calcium Flux Analysis

Human and rat NPCs were dissociated and plated on 15-mm poly-D-lysine-coated coverslips (Fisherbrand, Marshalltown, IA) as described previously at a density of $0.5–1 \times 10^6$/slide. Cells were loaded with 5 μM Fura-2 AM (Molecular Probes, Eugene, OR) in addition to Pluronic F-127 (Molecular Probes), to help reduce compartmentalization. After a 60-min loading period at 37°C in a 5% CO_2 incubator, the cells were washed with Locke's Buffer (154 mM NaCl, 3.6 mM $NaHCO_3$, 5.6 mM KCl, 1 mM $MgCl_2$, 5 mM HEPES, 2.3 mM $CaCl_2$, and 10 mM glucose) at pH 7.4 for a minimum of 30 min to allow for dye esterification. Coverslips were then mounted to a profusion chamber and buffer was injected via a pressure injection system. Groups of up to 20 NPCs were analyzed for intracellular calcium response to 100–500 ng/ml SDF-1α or IL-8. For T140 blocking, 10 nM T140 was added before and with SDF-1α stimulation. ATP (100 μM) was used as a positive control. The change in free Ca^{2+} was measured by monitoring the intensity of excitation emission at 510 nm in response to repeated sequential excitation at 340 and 380 nm using a digital camera (Photometrics, Huntington Beach, CA) or Photometer (Photon Technology International, London, Canada) coupled to an inverted Nikon TMD Diaphot epifluorescent microscope as described previously (Zheng et al., 1999). Data are presented as the relative ratio of fluorescence at 340 and 380 nm.

Chemotaxis Assay

The in vitro migration of human NPC in response to human SDF-1α was carried out using poly-D-lysine-coated polyvinylcarbonate-free membranes with 8–10 μm pore size in 96-well microchemotaxis chambers (NeuroProbe, Cabin John, MD). Protocols were carried out as described previously with some modifications (Klein et al., 2001). Briefly, 300 μl of Ex Vivo 15 containing 0.1% BSA with or without human SDF-1α (0–500 ng/ml) and 30 nM T140 were placed into the lower compartment. A 50-μl aliquot of dissociated NPC suspension (5×10^5 cells/ml) was added in the upper compartment of each well. For inhibition studies, cells were pretreated with 100 ng/ml of PTX for 2 hr at 37°C in a 5% CO_2-humidified incubator before dissociation. After incubation, the upper surfaces of the membranes were scraped free of cells and debris. The filter was then stained with Hoechst 33342 for 30 min. Cells that had migrated though the pore to the lower chamber and adhered to the lower surface of the filter were then counted in four microscopic fields per quadruplicate well, at 400× magnification. Results are expressed as mean number of cells migrating per four wells in four microscopic fields ± standard error of the mean (SEM).

Statistical Tests

For each experiment, samples were carried out in triplicate or quadruplicate and each treatment was repeated at least three times with cells from three individual donors. Data was analyzed as the mean ± standard deviation (SD) of the mean or SEM. The data was evaluated statistically by analysis of variance (ANOVA), followed by post-hoc Tukey test. Significance was considered to be less than 0.05.

RESULTS

CXCR4 Is Expressed in Rat Cortical NPCs

The phenotypes of rat cortical NPC were first identified by immunocytochemistry (Fig. 1). After being cultured in NPMM containing EGF and bFGF, the NPC phenotype was enriched. Passaged cells immunostained with nestin antibody (Fig. 1A), a marker for neuroepithelial stem cells (Lendahl et al., 1990; Messam et al., 2002). Less than 5% of cells exhibited immunostaining with MAP-2 (a specific neuronal marker) or GFAP (an astrocyte marker). BrdU staining suggested that the NPCs were undergoing self-renewal (Fig. 1B). After switching from NPMM to differentiation medium for 7 days, the NPC were allowed to differentiate into astrocytes (GFAP staining, Fig. 1C) and neurons (β-tubulin staining, Fig. 1D; MAP-2 staining, Fig. 1E; NeuN staining, Fig. 1F). No GalC-positive cells (oligodendrocyte marker, data not shown) were found in this culture system.

After confirming the high purity of our NPC culture, we then examined the expression of CXCR4 on rat cortical NPCs via immunocytochemistry. CXCR4 was found to be highly expressed by rat cortical NPCs (Fig. 1G). Double staining with nestin antibody showed that most nestin-positive NPCs expressed CXCR4 (data not shown). Reverse transcription PCR confirmed CXCR4 expression in rat cortical NPC cultures (data not shown). Interestingly, another α chemokine receptor, CXCR2, was also highly expressed in rat NPC (Fig. 1H). Conversely, other chemokine receptors, such as CXCR3 (receptor for IP-10), CCR5 (receptor for (MIP-1α) or regulated upon activation, normal T-cell expressed and presumably secreted [RANTES]), and CX3CR1 (receptor for fractalkine), seemed to be expressed in low levels as determined by immunocytochemistry (data not shown). After switching from NPMM to differentiation medium for 7 days, the NPCs were allowed to differentiate into neurons and astrocytes, still carrying CXCR4 expression (Fig. 1I, green). CXCR4 expression was also present on some undifferentiated NPCs (Fig. II). The expression of CXCR4 in neurons, however, seemed higher than that of astrocytes (Fig. 1I).

To confirm the expression of CXCR4 on rat cortical NPCs, we carried out radioligand binding. Competitive binding of [^{125}I] SDF-1α to NPC by increasing concentrations of unlabeled SDF-1α is demonstrated in Figure 2A. Unlabeled SDF-1α induced a dose-dependent inhibition of [^{125}I] SDF-1α binding on NPC with an IC_{50} value of 1.21 nM (total binding, 6064 ± 108 cpm/ml, with 50 pM [^{125}I] SDF-1α; nonspecific binding, 596 ± 18 cpm/ml with 100 nM of non-labeled SDF-1α presence; $n = 4$). T140, a CXCR4 antagonist (Tamamura et al., 1998, 2001), also displayed a dose-dependent inhibition of [^{125}I] SDF-1α binding on rat NPCs with an IC_{50} value of 0.9 nM.

SDF-1α Induces CXCR4 Signaling in Rat Cortical NPCs

Having demonstrated the expression of CXCR4 and SDF-1α binding on rat cortical NPC, we next examined signaling changes mediated by SDF-1α/CXCR4 interactions. On mature neurons, it has been shown previously that SDF-1α binding to CXCR4 receptors can mediate trimeric GTP-binding protein G inhibitory (Gi) protein activation including inhibition of adenylate cyclase and activation of PI hydrolysis (Zheng et al., 1999). To continue these studies, we carried out similar assays on rat cortical NPCs. As seen in Figure 2B, SDF-1α inhibited FSK-stimulated cAMP production in a dose-dependent manner. T140 (10 nM), a CXCR4 antagonist (Tamamura et al., 1998, 2001), blocks this change (Fig. 2B). Interestingly, IL-8 (ligand for CXCR2), IP-10 (ligand for CXCR3), RANTES, and fractalkine (ligand for CX3CR1), have shown no significant inhibition on FSK-stimulated cAMP production (Fig. 2D)

Next, we examined the effects of SDF-1α on IP_3 formation. As seen in Figure 2C, SDF-1α increased IP_3 formation in a dose-dependent manner. This could also be inhibited by T140. PTX, which uncouples heterotrimeric Gi proteins from G protein-linked seven-transmembrane receptors, could also inhibit this change, suggesting this effect is through activation of Gi/o.

SDF-1α Induces Calcium Flux in Depolarized Rat NPCs

Having shown the SDF-1α-mediated effect on cAMP accumulation and IP_3 formation, we next deter-

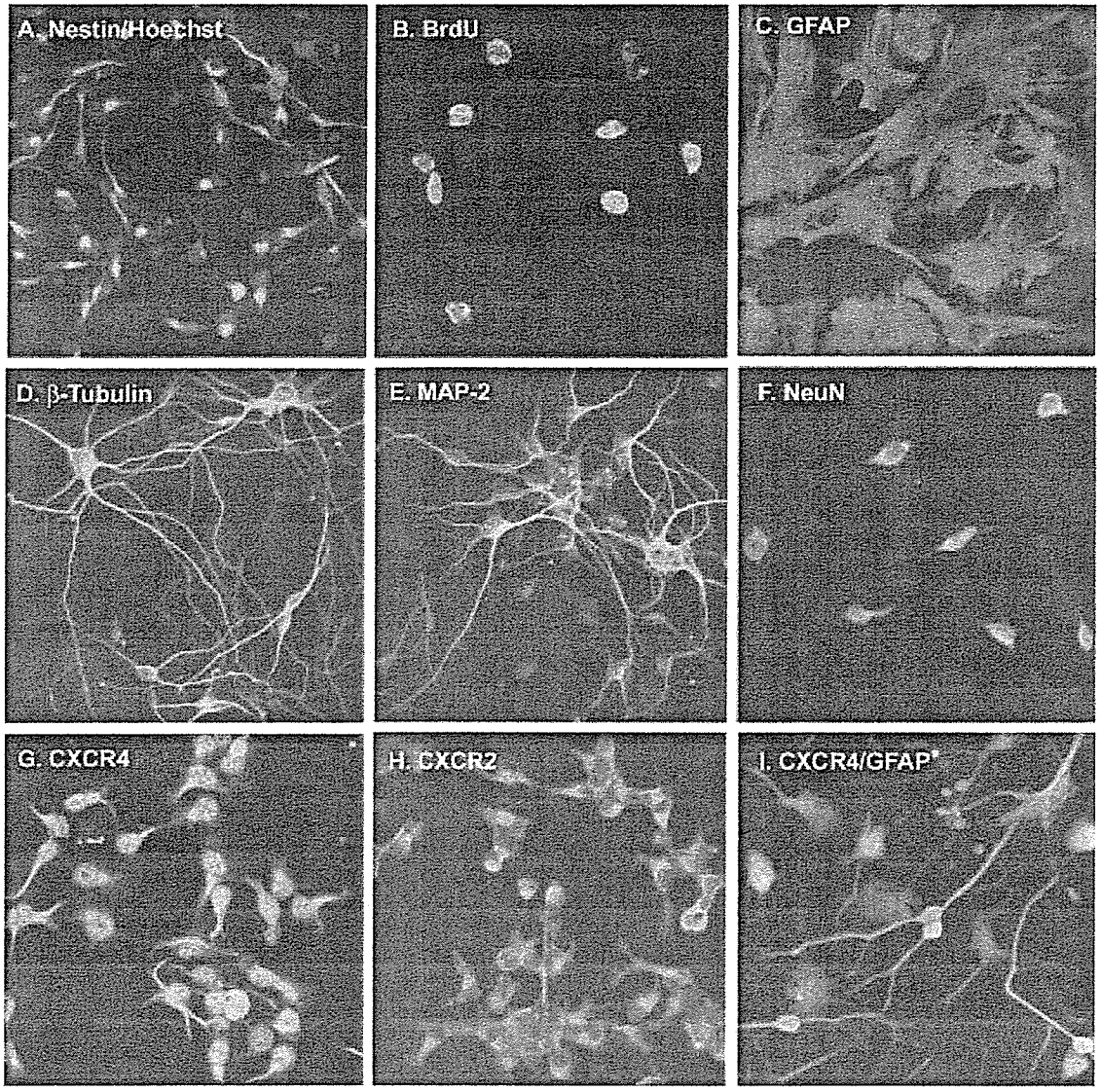

Fig. 1. Characterization and CXCR4 antigen expression on rat NPCs. Enriched NPCs were seeded in poly-D-lysine-coated chamber slides. Most cells were nestin+ and GFAP- (**A**). BrdU staining indicated that these NPCs were dividing cells (**B**). After being planted in 10% FBS for 7 days, the cells differentiated to astrocytes (**C**). They could also differentiate to neurons (**D**, β-tubulin; **E**, MAP-2; and **F**, NeuN) in Neurobasal/B27 media. Both CXCR4 and CXCR2 were expressed on rat cortical NPCs (**G**, CXCR4; **H**, CXCR2), CXCR4 were also expressed on differentiated neurons and astrocytes (CXCR4, green; GFAP, red; **I**). Original magnification in A is 200×, B–I are 400×. Results are representative of three independent experiments.

mined the effect of SDF-1α on calcium flux. In hematopoietic cells, SDF-1 signaling through CXCR4 induces a transient increase in intracellular calcium, which has been demonstrated to be essential for biological responses such as chemotaxis (Aiuti et al., 1997; Dutt et al., 1998). In rat cortical NPCs, the intracellular free Ca^{2+} response showed a substantial increase in the presence of SDF-1α (250 ng/ml, Fig. 3A). Interestingly, IL-8 (ligand for CXCR2, 250 ng/ml) can also induce a significant but smaller calcium response, as compared to SDF-1 treatment (Fig. 3B).

SDF-1α Activates MAP Kinases in Rat Cortical NPCs

To further examine the SDF-1α-mediated CXCR4 signaling in rat NPC, we focused our effort on the effects of SDF-1α on MAP kinases. In leukocytes, hematopoietic progenitor cells, and neural cells, SDF-1α has been shown to activate CXCR4 signaling and induce phosphorylation of several cellular proteins including MAP kinase (Aiuti et al., 1997; Dutt et al., 1998; Lazarini et al., 2000). Western blot analyses of ERK1/2, p38, JNK, and Akt (also referred to as protein kinase B [PKB]) phosphorylation were car-

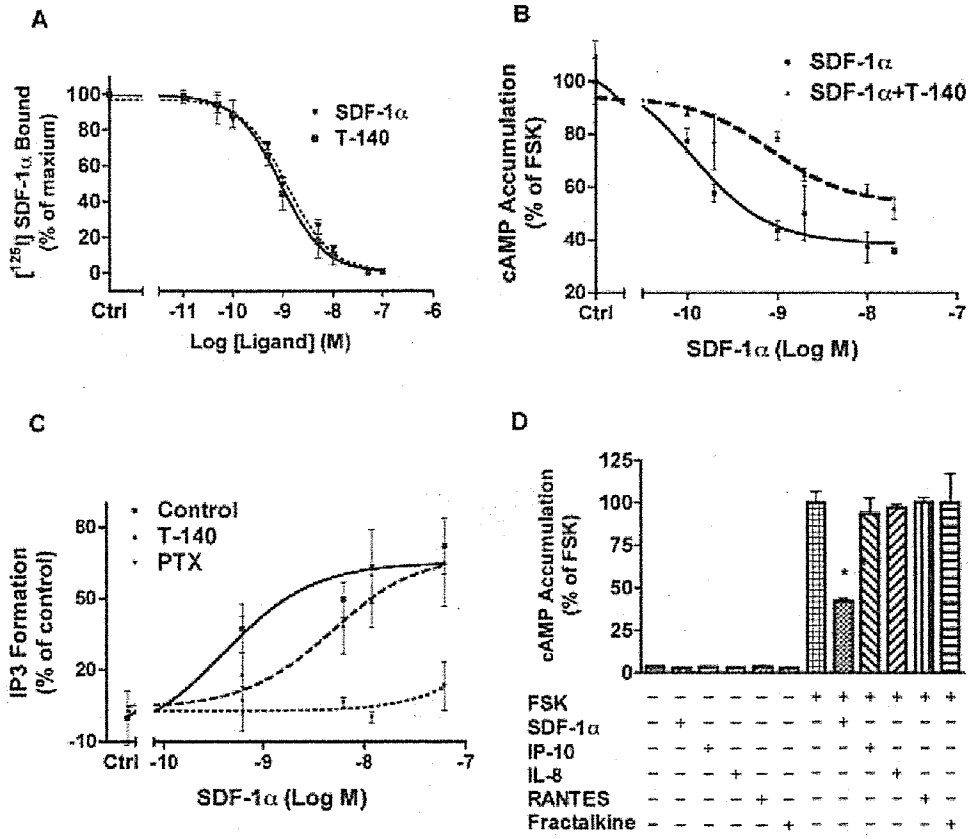

Fig. 2. Inhibition of [^{125}I] SDF-1α binding to rat NPCs by increasing concentrations of unlabeled SDF-1α and effects of SDF-1α on rat NPC cAMP accumulation and IP_3 hydrolysis. **A:** NPCs were incubated with 50 pM of [^{125}I] SDF-1α in the absence or presence of increasing concentrations of unlabeled SDF-1α or T140 in binding buffer (NPBM plus 1% of BSA) for 2 hr at room temperature. After incubation, cells were washed three times with binding buffer and lysed with 1% Triton X-100 in PBS. Lysates were transferred to glass test tubes and counted in a γ counter. Specific binding was calculated using total (containing no unlabeled SDF-1α) minus nonspecific binding (in the presence of 100 nM of unlabeled SDF-1α). The x-axis represents the concentration of unlabeled SDF-1α or T140 added. The y-axis represents the percent of counts seen as compared to the counts observed for the samples containing no unlabeled SDF-1α. **B:** SDF-1α could inhibit FSK-stimulated cAMP production in a dose-dependent manner and T140 (10 nM) blocks this change. IL-8, IP-10, RANTES, and fractalkine have shown no significant inhibition on FSK-stimulated cAMP production (**D**). SDF-1α increases IP_3 formation in a dose-dependent manner. This could also be inhibited by T140 and PTX (**C**). Results are expressed as average ± SD of triplicate samples and are representative of three independent experiments. $*P < 0.05$ in comparison to FSK alone.

ried out (Fig. 4). Immunoblot analysis with antibodies specific for the activated forms of ERK1/2, Akt, and JNK of rat cortical NPCs showed an increase in activation (phosphorylation) of these kinases after 1, 5, 10, and 30 min of treatment with SDF-1α (100 ng/ml, Fig. 4) or bFGF (25 ng/ml, positive control, data not shown). A two- to six-fold increase of ERK1/2, a two- to five-fold increase of Akt and a one- to two-fold increase of JNK as compared to controls was seen after SDF-1α treatment ($n = 3$, Fig. 4D–F) with a peak time at 5–10 min of stimulation. Finally, SDF-1α (100 ng/ml, 10 min) seemed to have no affect on p38 phosphorylation (data not shown). Together, these results demonstrate that SDF-1α can induce activation of ERK1/2, JNK, and Akt in rat NPC cultures and that the activation of these kinases by SDF-1α is essentially through activation of CXCR4.

CXCR4 Is Highly Expressed in Human Cortical NPCs

Having demonstrated CXCR4 expression and signaling in rat cortical NPCs, we next explored the pattern of CXCR4 expression and signaling in human cortical NPC. Similar to rat cortical NPCs, we first examined phenotypes of human cortical NPCs by immunocytochemistry (Fig. 5). After culturing in NPIM containing EGF, bFGF, and LIF, cells isolated from the developing cortex formed neurospheres after several passages (Fig. 5A) and expressed high levels of nestin (Fig. 5B). Most dissociated cells from these neurospheres were also immunostained with nestin antibody (Fig. 5C). After switching NPIM to differentiation medium for 7 days, NPCs were allowed to differentiate into neurons (Fig. 5D; β-tubulin staining, green; Fig. 5E; MAP-2 staining, green; Fig. 5F;

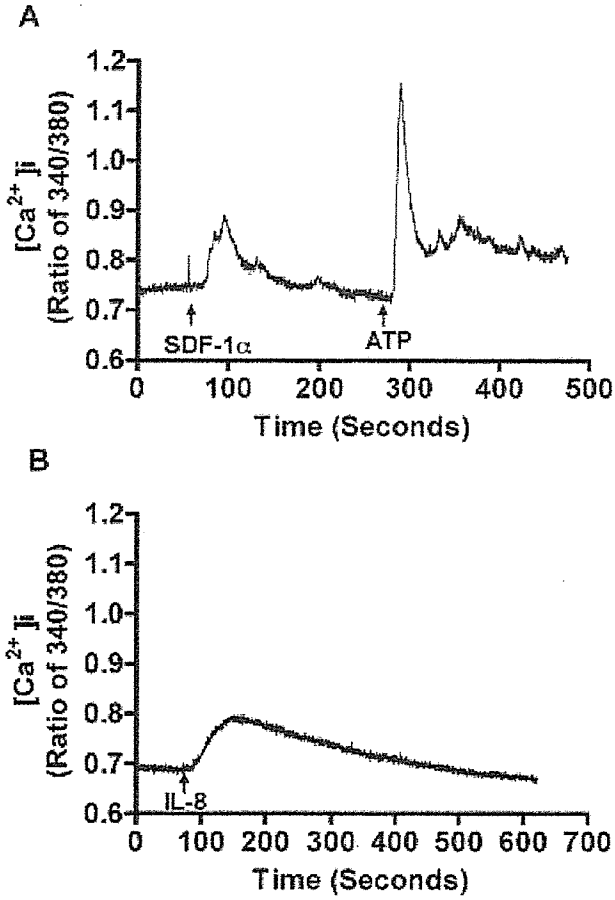

Fig. 3. SDF-1α and IL-8 induces calcium flux in rat NPCs. Chemokines (SDF-1α or IL-8) were applied on fura-2-loaded rat NPCs and groups of up to 20 NPCs were analyzed for intracellular calcium response by monitoring the intensity of excitation emission at 510 nm in response to repeated sequential excitation at 340 and 380 nm using a PTI imaging system coupled to an inverted Nikon TMD Diaphot epifluorescent microscope. The relative ratios of fluorescence at 340 and 380 nm were shown to represent intracellular free calcium. **A:** SDF-1α (250 ng/ml) was used. **B:** IL-8 (250 ng/ml) was used. Experiments are representative of three replicate assays carried out independently three times.

NeuN, green) and astrocytes (Fig. 5D–F; GFAP staining, red).

After confirming the high purity of our cultures, we next examined the expression of CXCR4 by immunocytochemistry. CXCR4 was highly expressed by human cortical NPCs in neurospheres and in dissociated format (Fig. 6B,E). Double staining with nestin antibody showed that most nestin-positive NPCs expressed CXCR4 (Fig. 6C,F). Similar to rat NPCs, after switching from NPIM to differentiation medium for 7 days, the NPCs were allowed to differentiate into neurons and astrocytes and CXCR4 expression (Fig. 6G,I; green) remained in neurons and astrocytes. CXCR4 expression in neurons seemed higher than that in astrocytes (Fig. 6I).

To further confirm the expression of CXCR4 on human cortical NPCs, radioligand binding was also carried out. As demonstrated in Figure 7A, unlabeled SDF-1α induced a dose-dependent inhibition of [^{125}I] SDF-1α binding on human cortical NPCs with an IC_{50} value of 3.27 nM (total binding, 12,688 ± 1,248 cpm/ml, with 50 pM [^{125}I] SDF-1α; nonspecific binding; 1,143 ± 108 cpm/ml with 100 nM of non-labeled SDF-1α; n = 3). T140 also displayed a dose-dependent inhibition of [^{125}I] SDF-1α binding on human cortical NPCs with an IC_{50} value of 1.84 nM. These results confirmed high levels of CXCR4 expression on human cortical NPCs.

SDF-1α Induces CXCR4 Signaling in Human Cortical NPCs

Having demonstrated the expression of CXCR4 and SDF-1α binding, we next repeated our previously described signaling studies on human cortical NPCs. As shown in Figure 7B, human cortical NPCs exhibit SDF-1α-mediated inhibition of FSK-stimulated cAMP production. T140 (10 nM) and PTX (100 ng/ml) blocked this change (Fig. 7B). These results show that both rat and human cortical NPCs share similar signaling characteristics. Fractalkine (ligand for CX3CR1), IL-8 (ligand for CXCR2), and IP-10 (ligand for CXCR3) showed no significant inhibition on FSK-stimulated cAMP production (Fig. 7C).

Having shown SDF-1α mediated similar effects on cAMP accumulation in human cortical NPCs, we next determined the effect of SDF-1α on calcium flux. Human cortical NPCs showed similar trends to rat NPCs in all areas. In human cortical NPCs, intracellular free Ca^{2+} response exhibited a substantial increase in the presence of SDF-1α (250 ng/ml, Fig. 8A). This calcium flux response was T140 sensitive (Fig. 8B), suggesting that SDF-1α was acting via CXCR4. ATP (100 μM) mediated a similar calcium response, in NPC with or without T140 pretreatment (Fig. 8A,B). Interestingly, IL-8 (ligand for CXCR2, 250 ng/ml) treatment induced a significant but smaller calcium response compared to SDF-1 treatment (Fig. 8C).

To further examine SDF-1α-mediated CXCR4 signaling in human cortical NPCs, we again measured the effect of SDF-1α on MAP kinases and Akt (Fig. 9). Western blot analysis with antibodies specific for activated forms of ERK1/2, JNK, and Akt showed increased activation (phosphorylation) of these kinases at 1, 5, or 10 min of treatment with SDF-1α (100 ng/ml) with a peak time at 10 min of stimulation. A one- to three-fold increase of ERK1/2, a 2.3- to 2.6-fold increase of Akt and a 2.4 to 2.5-fold increase of JNK as compared to controls was seen after SDF-1α treatment (100 ng/ml for 10 min; n = 3; Fig. 9E–H). Again, T140 and PTX both inhibited SDF-1α-mediated activation of ERK1/2, JNK, and Akt in these cultures (Fig. 9). SDF-1α (100 ng/ml, 10 min) seemed to have no effect on p38 phosphorylation (data not shown). Taken together, these results demonstrated that SDF-1α induced similar activation of ERK1/2, JNK, and Akt in both human and rat cortical NPC cultures and that

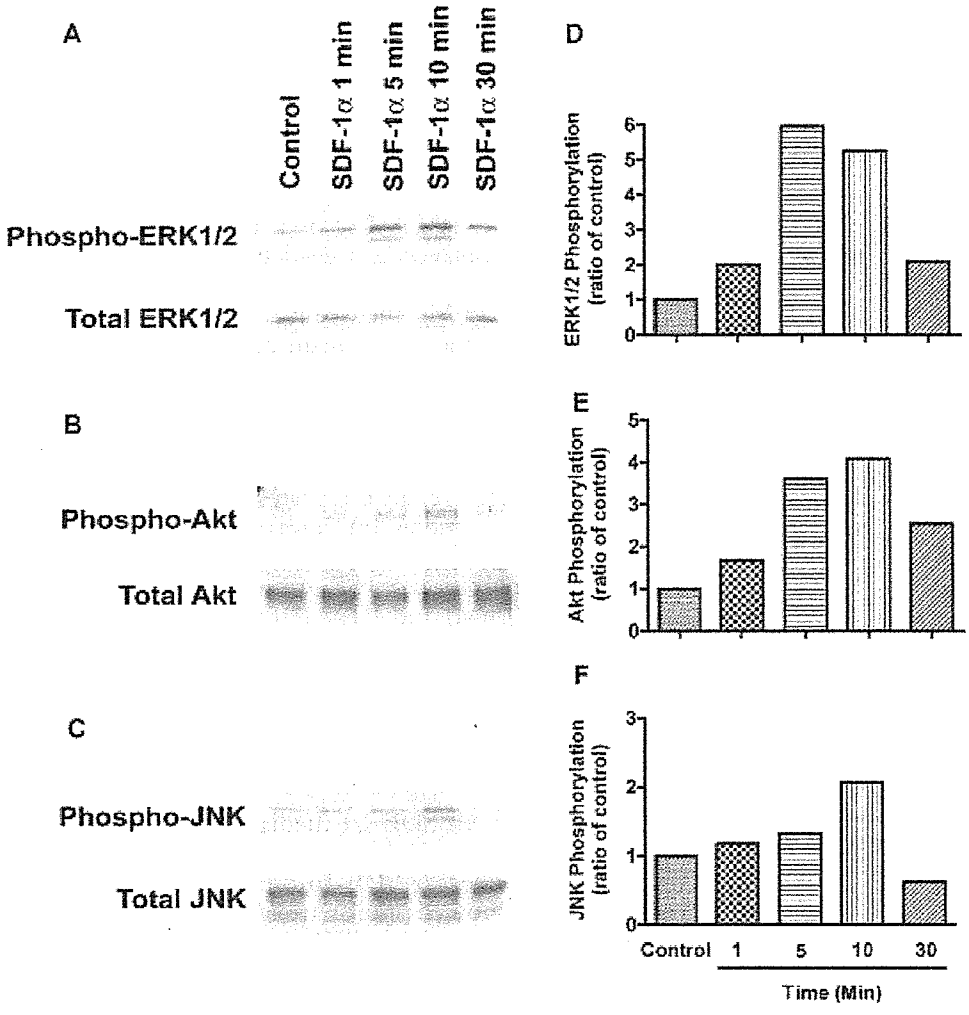

Fig. 4. Effects of SDF-1α on ERK1/2, Akt, and JNK in neural progenitor cell cultures. Western blots of total cell lysates were obtained from rat NPC cultures treated with 100 ng/ml SDF-1α for 1, 5, 10 and 30 min. Antibodies selectively recognizing the activated and total form of ERK1/2, Akt, and JNK were used. Rat cortical NPCs showed increased activation (phosphorylation) of ERK1/2 (**A**), Akt (**B**), and JNK (**C**). Data shown as the ratio of phosphorylated and total (**D–F**). Results are representative of three independent experiments.

activation of these kinases by SDF-1α was essentially through activation of CXCR4.

SDF-1α Induces CXCR4-Mediated Chemotaxis in Human Cortical NPCs

Having shown SDF-1α-mediated CXCR4 signaling in human cortical NPCs, we next determined the functional role of SDF-1α on NPC recruitment through an in vitro chemotaxis assay. SDF-1 has been suggested to be a potent chemoattractant for isolated striatal precursors (Stumm et al., 2003) or progenitors derived from rat cerebellum (Klein et al., 2001). To continue these studies, we investigated whether these cells respond to SDF-1α with directed migration, using a chemotactic chamber assay. Human NPCs migrated in a dose-dependent manner toward SDF-1α with a peak response at 100–500 ng/ml (Fig. 10A). T140 (30 nM) and PTX (100 ng/ml) both inhibited SDF-1α-mediated chemotactic response (Fig. 10B). In addition, NPCs migrated toward SDF-1α only in response to a chemical gradient, as their migration was not increased significantly when identical concentrations of SDF-1 were added to the upper and lower chemotaxis chambers (data not shown).

DISCUSSION

We demonstrated that CXCR4 was highly expressed in both rat and human cortical NPCs. SDF-1α, a CXCR4 ligand, activated a wide range of Gi protein-linked signaling pathways resulting in diminished cAMP, increases in IP_3 formation and elevation of intracellular calcium. Moreover, SDF-1α also induced increased activation of ERK1/2, Akt, and JNK, all of which are critical steps for inducing cell proliferation and migration. Notably, SDF-1α can induce human NPC chemotaxis in vitro, suggesting that CXCR4 plays a functional role in NPC migration. PTX and the CXCR4 antagonist T140 both halted these functional changes. Furthermore, the similar patterns in CXCR4 expression and signaling in both rat and human cortical NPCs indicates that SDF-1/CXCR4 engagement is similar among species. These observations suggest that CXCR4 plays an important role in regulating neurogenesis.

Previous studies have demonstrated that SDF-1 and CXCR4 signaling play critical roles in neuronal development (Ma et al., 1998; Zou et al., 1998; Lazarini et al., 2000; Lu et al., 2001; Stumm et al., 2003). In mice, NPC

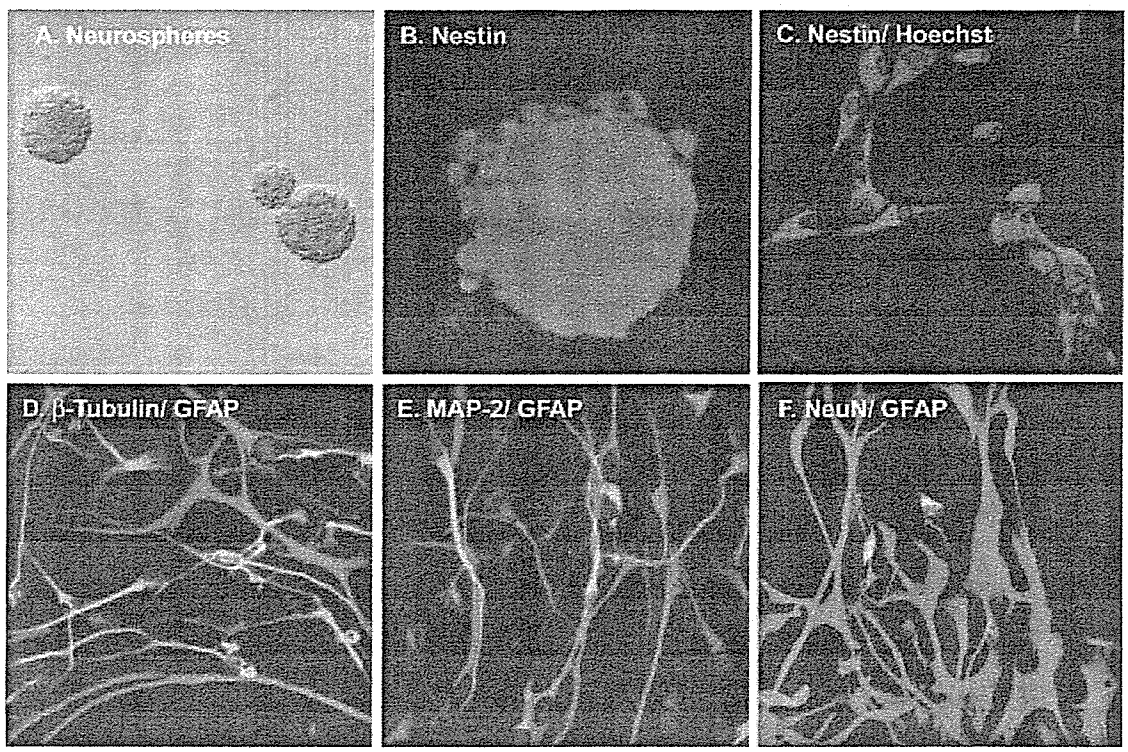

Fig. 5. Culture of human cortical NPCs. Cells were isolated and grown in NPIM as described. Neurospheres formed after several passages (**A**). Immunocytochemical staining showed that most cells within the growing spheres were nestin+ cells (**B**); this was also shown in the dissociated cells (**C**). The dissociated cells were plated in poly-D-lysine-coated chamber slides in Neurobasal media with B27 for 7 days to induce differentiation. Cells derived from neurospheres were differentiated to neurons (**D**, β-tubulin, green; **E**, MAP-2; or **F** NeuN) and astrocytes (D–F, GFAP, red). No oligodendrocytes (GalC-positive cells) were found in this culture system. Results are representative of three independent experiments.

migration and survival requires SDF-1/CXCR4 interactions (Molyneaux et al., 2003). Deletions of the genes encoding for SDF-1 or CXCR4 are lethal for mice soon after birth, with severe abnormalities affecting neuronal precursor migration in cerebellum (Ma et al., 1998; Zou et al., 1998), hippocampal dentate gyrus (Lu et al., 2001; Bagri et al., 2002), and neocortex (Stumm et al., 2003). Our studies extended these in vivo and in vitro observations by further characterizing SDF-1 and CXCR4 signaling in purified NPC cultures derived from both rat and human cortexes. We chose NPCs derived from the cortex as our working model due to the recent progress and realization of the importance of SDF-1 and CXCR4 in cortical development, especially interneuron migration in the developing neocortex (Lazarini et al., 2000; Stumm et al., 2003). Lazarini et al. (2000) first reported that CXCR4 expression and activation of ERK by SDF-1 on rat cortical progenitors implicated the importance of CXCR4 in cortical neural development. This study was developed further by a report showing that SDF-1α was highly expressed in the embryonic leptomeninx and that SDF-1α was a potent chemoattractant for isolated striatal precursors (Stumm et al., 2003). In addition, it has been shown that CXCR4 is present in early-generated Cajal-Retzius cells of the cortical marginal zone. Although mice with a null mutation in CXCR4 or SDF-1 show severe disruption of interneuron placement and proliferation, the submeningeal positioning of Cajal-Retzius cells remains unaffected (Stumm et al., 2003). Examining CXCR4 expression and its function on rat and human cortical NPCs could thus further our understanding of the physiologic function of this receptor in cortical development.

In this study, E15 rat embryos were chosen for culture of cortical NPC (Hazel and Muller, 1997). Notably, the expression and function of CXCR4 at different embryo stages is different. The onset of mRNA expression is around E9 and there are high levels of mRNA expression in the neuroepithelium at E14 and E16 (Jazin et al., 1997). Based on the literature and our unpublished data, E15 brain neural progenitors are a group of stem and progenitor cells (Davis and Temple, 1994; Lazarini et al., 2000). After being cultured in growth factor-enriched media, most cells express nestin instead of neuronal or glia cell markers, making this culture an enriched multipotent stem and progenitor cell culture. It would be interesting to determine the signaling and function of NPCs derived from different embryonic stages. Future studies on this topic would certainly generate additional important information.

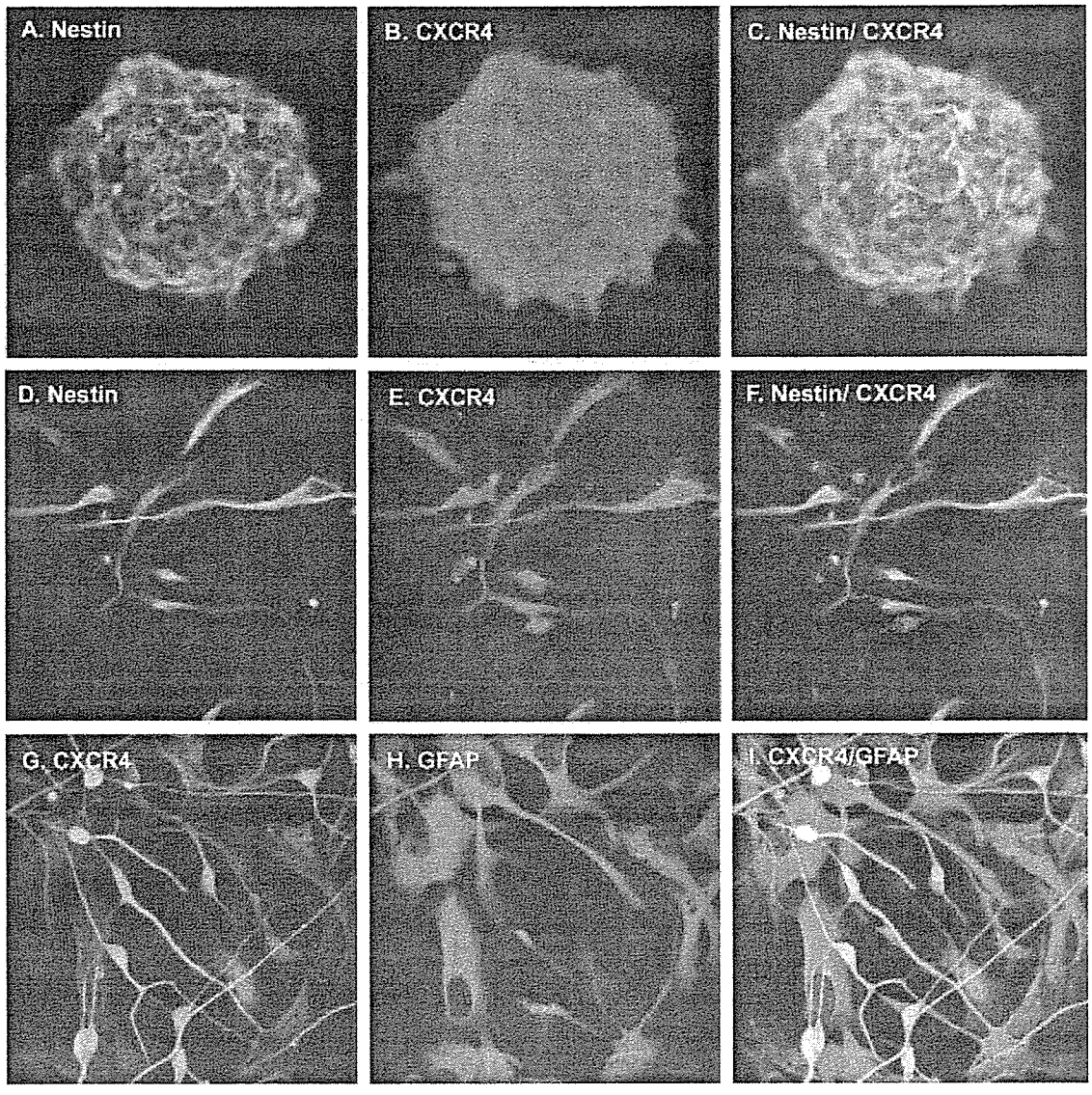

Fig. 6. Characterization and CXCR4 antigen expression on human cortical NPCs. Cells were isolated and grown in NPIM as described. CXCR4 was highly expressed by human cortical NPCs, both in neurospheres (**B**) and dissociated format (**E**). Double staining with nestin antibody showed that CXCR4 is expressed on the nestin+ cells (**C, F**). CXCR4 was also highly expressed by differentiated cells (**G**). Double staining with GFAP showed that small amount of CXCR4 is expressed on astrocytes whereas most neurons express CXCR4 (**I**). Results are representative of three independent experiments.

It has been suggested that three important steps are involved in neurogenesis and NPC regulation: direct migration, proliferation, and differentiation (Fallon et al., 2000). Whether SDF-1/CXCR4 interaction is involved in all three steps is not well known; however, it has been well documented that SDF-1/CXCR4 signaling regulates NPC migration in cerebellum (Ma et al., 1998; Zou et al., 1998), hippocampal dentate gyrus (Bagri et al., 2002; Lu et al., 2001), and neocortex (Stumm et al., 2003). For example, it has been shown that NPCs isolated from E15 cerebella, migrate in a dose-dependent manner toward SDF-1 (Klein et al., 2001). Additionally, this SDF-1α-induced chemotaxis was blocked by PTX and by AMD3100, a CXCR4 antagonist, suggesting receptor-mediated signaling in this process (Klein et al., 2001). Consistent with this report, our results also show that SDF-1 induced human cortical NPC migration though CXCR4 activation (Fig. 10), further implicating the important role of CXCR4 in NPC migration. In the same report, the authors also demonstrated that SDF-1α acts synergistically with sonic hedgehog to promote cerebellar granule precursor cell proliferation (Klein et al., 2001). Although there are no direct reports on effects of SDF-1α on NPC differentiation, it has been suggested that SDF-1α may play a role in the increase of neurite outgrowth in neuronal cultures (Langford et al., 2002). Considering the

possible presence of NPC contamination in the primary neuronal culture (Peng et al., unpublished observation), this result could be the effect of SDF-1α on NPCs as opposed to the primary cultures. Notably, studies into the abilities and possible mechanisms of SDF-1/CXCR4 interactions on NPC directed migration, proliferation and differentiation would provide valuable information for the effect of SDF-1/CXCR4 in neurogenesis. Furthermore, linking individual signaling pathways to each possible phenotype of CXCR4 on NPC function would provide insightful information regarding the molecular mechanism of CXCR4 regulation on NPCs.

Certainly, SDF-1-mediated CXCR4 intracellular signaling may regulate these responses, differentially or concurrently. An in vitro assay has shown that CXCR4-directed cellular migration was blocked by PD98059, a MAP kinase pathway inhibitor, suggesting the role of this signaling pathway in NPC migration (Klein et al., 2001). Our results further support this observation because ERK1/2 phosphorylation (activation) can be induced in both rat and human NPCs (Figs. 4 and 9). It has been suggested also that SDF-1-mediated calcium responses are important for CXCR4-mediated cellular migration and that SDF-1/CXCR4 interactions are important for CXCR4-mediated cellular proliferation (Klein et al., 2001). In this study, SDF-1-CXCR4 interaction-mediated enhancement of NPC proliferation was blocked by forskolin, a protein kinase A (PKA) activator. This observation suggests that SDF-1α-mediated inhibition of cAMP accumulation and PKA may be instrumental for its proliferative effect on NPCs (Klein et al., 2001). Our results support this notion because SDF-1α inhibited forskolin-stimulated cAMP accumulation in both rat and human cortical NPCs (Figs. 2 and 7). Our results demonstrated also that Akt and JNK phosphorylation are induced by SDF-1α in both rat and human NPC (Figs. 4 and 9). Although Akt activation has been linked to cellular proliferation and survival (Andjelic et al., 2000; Lataillade et

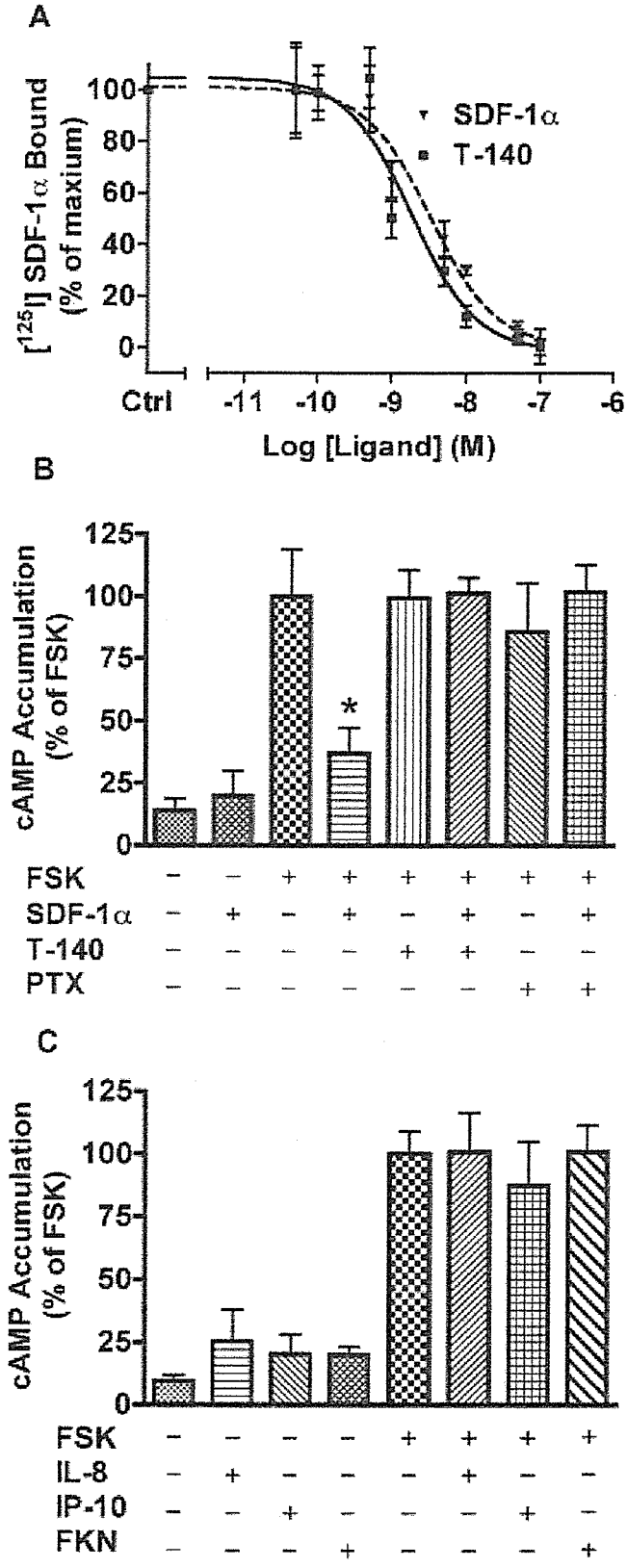

Fig. 7. CXCR4 binding and signaling on human NPCs. **A:** Inhibition of [^{125}I] SDF-1α binding to human NPCs are shown with increasing concentrations of unlabeled SDF-1α or T140. NPC were incubated with 50 pM of [^{125}I] SDF-1α in the absence or presence of increasing concentrations of unlabeled SDF-1α or T140 in binding buffer (NPIM plus 1% BSA) for 2 hr at room temperature. After incubation, cells were washed three times with binding buffer and lysed with 1% Triton X-100 in PBS. Lysates were transferred to glass test tubes and counted in a γ counter. Specific binding was calculated using total (containing no unlabeled SDF-1α) minus nonspecific binding (in the presence of 100 nM of unlabeled SDF-1α). The x-axis represents the concentration of unlabeled SDF-1α or T140 added. The y-axis represents the percent of counts seen as compared to the counts observed for the samples containing no unlabeled SDF-1α. **B, C:** Effects of SDF-1α on human cortical NPCs cAMP accumulation are demonstrated. SDF-1α could inhibit FSK-stimulated cAMP production. T140 (10 nM) and PTX (100 ng/ml) block this change (B). Fractalkine, IL-8 and IP-10 have shown no significant effect (C). Results are expressed as average ± SD of triplicate samples and are representative of three independent experiments. $*P < 0.05$ in comparison to FSK alone.

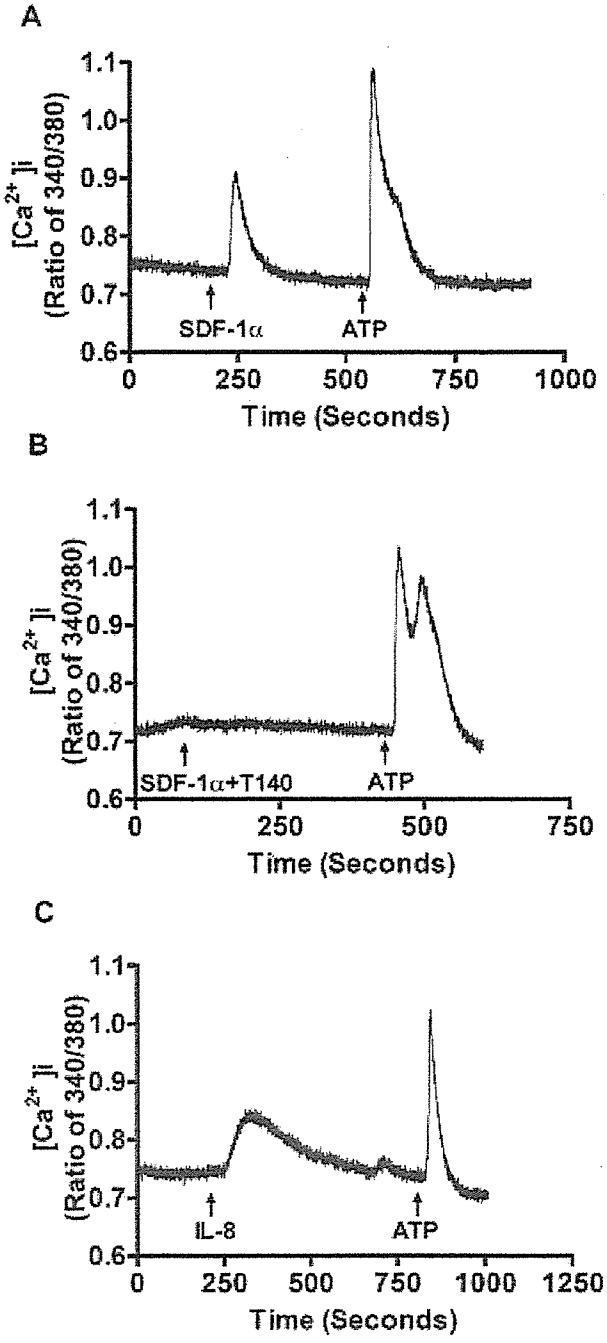

Fig. 8. SDF-1α and IL-8 induces calcium flux in human NPCs. Chemokines (SDF-1α or IL-8) were applied on fura-2-loaded rat NPCs and intracellular calcium was measured by monitoring the intensity of excitation emission at 510 nm in response to repeated sequential excitation at 340 and 380 nm using a PTI imaging system coupled to an inverted Nikon TMD Diaphot epifluorescent microscope. The relative ratio of fluorescence at 340 and 380 nm were shown to represent intracellular free calcium. **A:** SDF-1α (250 ng/ml) was used. In replicate cultures (**B**), NPCs were pretreated with T140 (10 nM) and then stimulated with SDF-1α (250 ng/ml) in the presence of T140 (10 nM). **C:** IL-8 (250 ng/ml) was used. The experiments are representative of three replicate assays carried out three times independently.

al., 2002), the exact outcome of this signaling pathway in NPCs is currently unknown. Notably, JNK activation has been suggested recently to play a role in neuronal survival and differentiation (Coffey et al., 2000). It is thus certainly worthwhile to further elucidate the roles of these signaling pathways in regulating NPC migration, proliferation, and differentiation. Because there is cross talk between signaling pathways such as IP_3 formation, calcium release, and PKA, the exact role of these signaling molecules in regulating NPC complex function requires further detailed investigation.

It is interesting to note that T140 and PTX have some effect on JNK and ERK phosphorylation, although neither shows significant changes as compared to the control (Fig. 9). The reason for this phenomenon remains unknown. One explanation for such small changes by PTX could be possible endogenous SDF-1 production from NPCs. It has been shown that neurons and astrocytes are the source of SDF-1α in vitro and in vivo (Zheng et al., 1999; Langford et al., 2002; Rostasy et al., 2003); therefore, NPCs could also produce SDF-1α. The small inhibitory effect of PTX could block this potential endogenous SDF-1 effect; however, this hypothesis certainly requires further investigation.

The high expression and function of CXCR4 on NPCs could also provide new avenues of investigation in human immunodeficiency virus (HIV)-1-associated neurologic disease. HIV-1-associated dementia (HAD) has affected approximately 20% of infected adults and 50% of infected children before the era of highly active antiretroviral therapy (Epstein and Gelbard, 1999; McArthur et al., 1999). HAD and HIV-1 encephalitis (HIVE), the histopathologic correlate of HAD (Glass et al., 1993) are both examples of HIV-1-associated neurologic diseases. HIVE is characterized by the presence of HIV-infected and immune-activated mononuclear phagocytes (MPs; monocytes, macrophages and microglia) and its association of neuronal injury and death in the brain (Glass et al,. 1995; Lipton and Gendelman, 1995; Strizki et al., 1996; Gendelman et al., 1997; He et al., 1997; Masliah et al., 1997; Conant et al., 1998; Gabuzda et al., 1998; Nath and Geiger, 1998; Kolson and Gonzalez-Scarano, 2000; Kaul et al., 2001). It is believed that MPs could secrete cytotoxic factors and viral proteins, such as HIV-1 gp120, that damage or destroy neurons (Hesselgesser et al., 1998; Meucci et al., 1998; Kaul and Lipton, 1999; Zheng et al., 1999; Bachis et al., 2003). Such processes can be amplified by the interaction with other brain cells such as astrocytes (Gendelman et al., 1997; Gabuzda et al., 1998; Nath and Geiger, 1998). It has also been suggested that SDF-1α is upregulated in the brain of patients with HIVE (Langford et al., 2002; Rostasy et al., 2003). SDF-1 is expressed constitutively by neurons and astrocytes, which is upregulated during inflammation processes (Zheng et al., 1999; Langford et al., 2002; Rostasy et al., 2003). Interestingly, SDF-1 (1–67 amino acids [aa]) can be cleaved by active matrix metalloproteinase-2 produced by HIV-1-infected macrophages and converted to a highly neurotoxic pro-

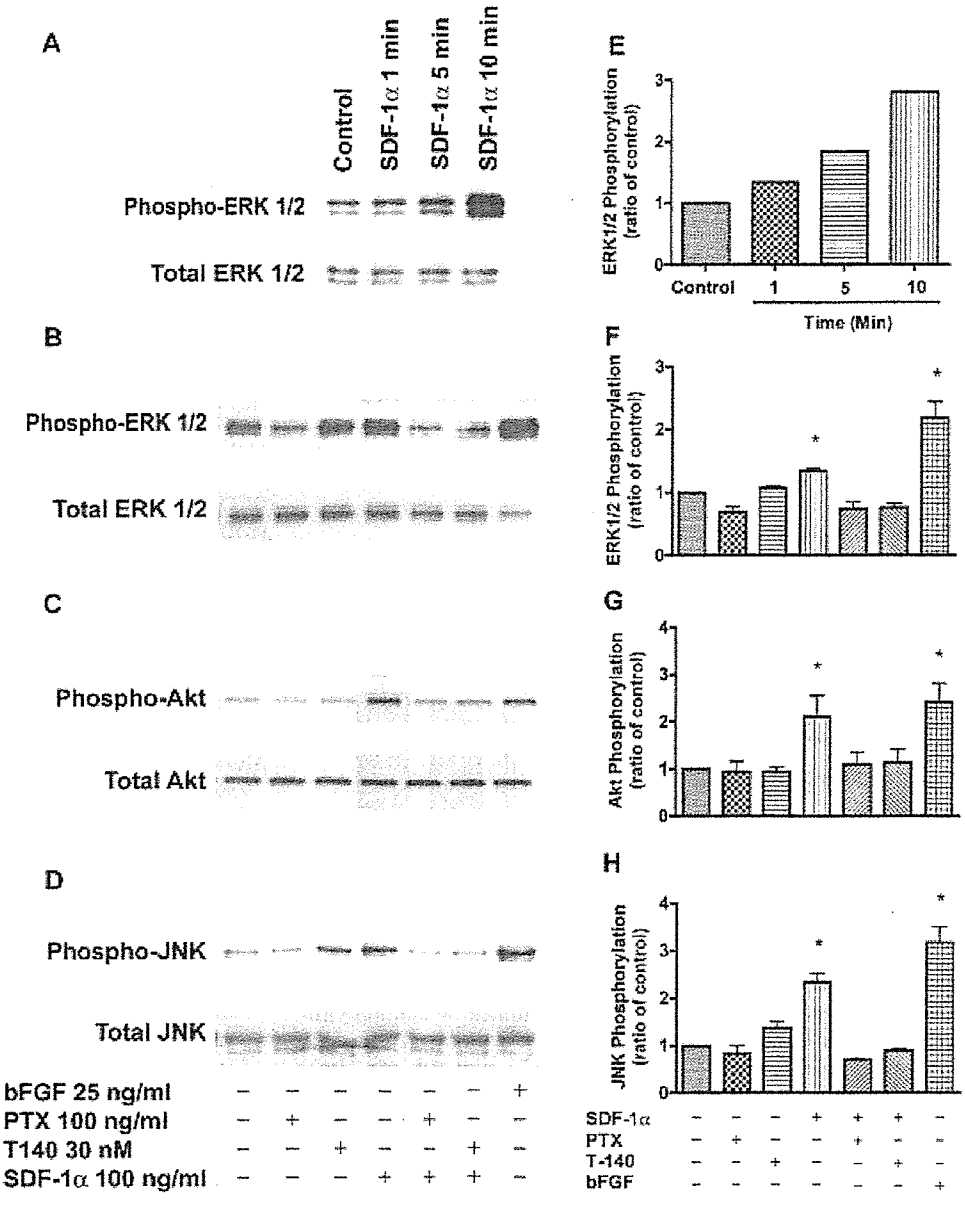

Fig. 9. Effects of SDF-1α on ERK1/2, Akt, and JNK phosphorylation in human NPCs. Human cortical NPCs were deprived of NPIM for 5 hr before being treated with 100 ng/ml SDF-α for 1, 5, or 10 min. Western blot analysis with antibodies specific for the activated forms of ERK1/2, JNK, and Akt showed increased activation (phosphorylation) of these kinases at 1, 5, or 10 min of treatment with a peak time at 10 min of stimulation (**A**). A one- to threefold increase of ERK1/2 (A, **B**), a 2.3- to 2.6-fold increase of Akt (**C**) and a 2.4- to 2.5-fold increase of JNK (**D**) as compared to controls was seen after SDF-1α treatment (100 ng/ml, 10 min, $n = 3$, **E–H**). For blocking, cells were treated with 30 nM T140 for 30 min and PTX for 5 hr. A–D: Representative autoradiograph. Data shown as the ratio of phosphorylated and total (E–H). Results are representative of three independent experiments. $*P < 0.05$ in comparison to control.

tein, SDF-1 (5–67 aa) (Zhang et al., 2003). Upregulated SDF-1 or SDF-1 fragments during HAD thus could affect NPC function, eventually affecting neurogenesis and neuronal repair. On the other hand, HIV-1 gp120, released by infected cells in the brain, could potentially bind CXCR4 on NPCs and affect their function, which might be similar to some of the mature neurons (Hesselgesser et al., 1998; Meucci et al., 1998; Kaul and Lipton, 1999; Zheng et al., 1999; Bachis et al., 2003; Bodner et al., 2003). Notably, these questions and hypothesis warrant thorough investigation.

It is interesting to note that other chemokine receptors such as CXCR2, CX3CR1, and CCR5 are expressed at different levels by both rat and human cortical NPCs. Only a small, insignificant cAMP signaling was observed for CXCR2, CX3CR1 and CCR5 ligands (Figs. 2 and 7). We believe this could be because of the lower expression rate of these chemokine receptors. Interestingly, IL-8 can also induce a significant but smaller calcium responses, as compared to SDF-1 treatment, in both rat and human NPCs (Figs. 3 and 8). The exact pattern and function of these chemokine receptors in neuronal development and neurogenesis require further confirmation and investigation. Notably, IL-8, fractalkine, and MIP-1α, ligands for chemokine receptors CXCR2, CX3CR1, and CCR5, respectively, were shown to be neuroprotective in the CNS (Meucci et al., 1998, 2000; Kaul and Lipton, 1999; Coughlan et al., 2000; Tong et al., 2000; Zheng et al., 2001). In addition, the levels of IL-8 and fractalkine are higher in HAD patients as compared to HIV-1 infected

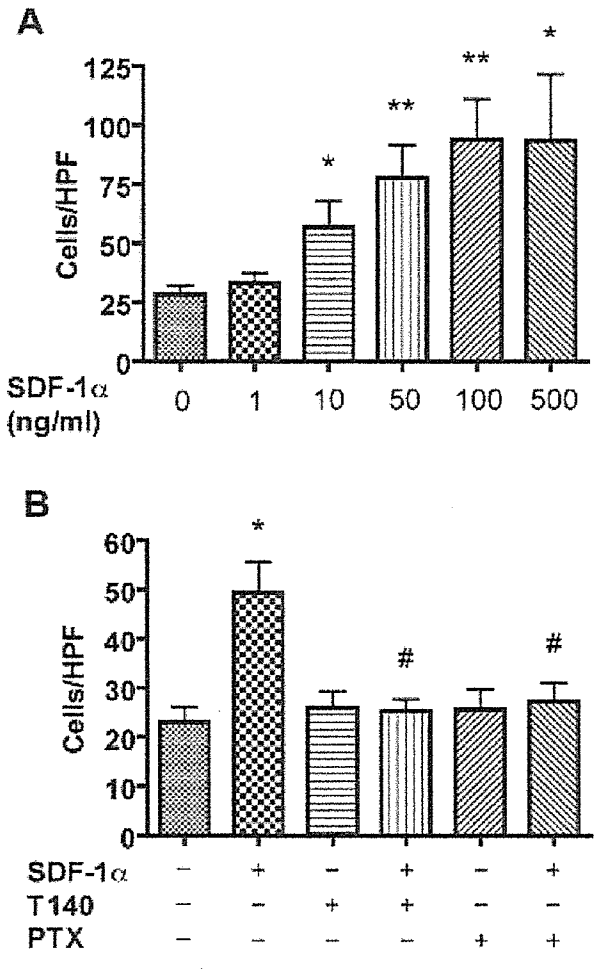

Fig. 10. Effects of SDF-1α on migration of human NPCs. The chemotactic response of human NPCs was determined by counting migrating cells per high-powered field (cells/HPF ± SEM) in four fields from each quadruplicate well. Human NPCs migrated in a dose-dependent manner toward SDF-1α with a peak response at 100–500 ng/ml (**A**). The chemotactic response to 50 ng/ml SDF-1α was abolished by pretreated of cells with PTX or T140 (**B**). Data shown is represents two separate experiments where each data point was carried out in quadruplicate. $*P < 0.05$; $**P < 0.01$ in comparison to control. $\#P < 0.05$ in comparison to SDF-1α.

patients with no neurologic symptoms (Tong et al., 2000; Zheng et al., 2001; Erichsen et al., 2003). Certainly, in-depth studies on SDF-1α/CXCR4 and other chemokines and their receptors on NPC signaling may shed insights into the roles of these chemokines and their receptors in neurogenesis and repair. This effort would also provide valuable information on the pathogenesis of other neurodegenerative disorders such as HAD and Alzheimer's disease where chemokines have been reported to play roles in neuronal dysfunction (Xia and Hyman, 1999; Ransohoff et al., 2003; Tran and Miller, 2003).

In summary, the chemokine SDF-1 and its receptor CXCR4 have been shown previously to play critical roles in brain development and neurogenesis. CXCR4 is highly expressed by rat and human NPCs, and SDF-1α cell signaling is mediated through CXCR4. We provide in the present study a preliminary characterization of SDF-1α-CXCR4 interactions in NPCs. Such observations may serve to further our understanding of SDF-1 and CXCR4 interactions in CNS development and aid in the better understanding of the pathogenesis of neurodegenerative disorders.

ACKNOWLEDGMENTS

We thank Drs. H. Gendelman, A. Ghorpade, L. Ryan, R. Cotter, T. Ikezu, M. Thomas (CCND), and E. Major (NINDS/NIH) for scientific support and fruitful discussion. We also thank L. Wu, A. Lopez, J. Zhao, D. Xu, N. Erdmann, and A. Cheloha for technical support for this work. Ms. R. Taylor contribution for providing outstanding support in assembling the work for publication is also appreciated.

REFERENCES

Aiuti A, Webb IJ, Bleul C, Springer T, Gutierrez-Ramos JC. 1997. The chemokine SDF-1 is a chemoattractant for human CD34+ hematopoietic progenitor cells and provides a new mechanism to explain the mobilization of CD34+ progenitors to peripheral blood. J Exp Med 185:111–120.

Alvarez-Buylla A, Garcia-Verdugo JM. 2002. Neurogenesis in adult subventricular zone. J Neurosci 22:629–634.

Alvarez-Buylla A, Seri B, Doetsch F. 2002. Identification of neural stem cells in the adult vertebrate brain. Brain Res Bull 57:751–758.

Andjelic S, Hsia C, Suzuki H, Kadowaki T, Koyasu S, Liou HC. 2000. Phosphatidylinositol 3-kinase and NF-kappa B/Rel are at the divergence of CD40-mediated proliferation and survival pathways. J Immunol 165: 3860–3867.

Bachis A, Major EO, Mocchetti I. 2003. Brain-derived neurotrophic factor inhibits human immunodeficiency virus-1/gp120-mediated cerebellar granule cell death by preventing gp120 internalization. J Neurosci 23: 5715–5722.

Bagri A, Gurney T, He X, Zou YR, Littman DR, Tessier-Lavigne M, Pleasure SJ. 2002. The chemokine SDF1 regulates migration of dentate granule cells. Development 129:4249–4260.

Berson JF, Long D, Doranz BJ, Rucker J, Jirik FR, Doms RW. 1996. A seven-transmembrane domain receptor involved in fusion and entry of T-cell-tropic human immunodeficiency virus type 1 strains. J Virol 70: 6288–6295.

Bodner A, Toth PT, Oh SB, Lu M, Tran PB, Chin RK, Ren D, Miller RJ. 2003. CD4 dependence of gp120IIIB-CXCR4 interaction is cell-type specific. J Neuroimmunol 140:1–12.

Brelot A, Heveker N, Pleskoff O, Sol N, Alizon M. 1997. Role of the first and third extracellular domains of CXCR-4 in human immunodeficiency virus coreceptor activity. J Virol 71:4744–4751.

Broxmeyer HE, Kim CH. 1999. Regulation of hematopoiesis in a sea of chemokine family members with a plethora of redundant activities. Exp Hematol 27:1113–1123.

Coffey ET, Hongisto V, Dickens M, Davis RJ, Courtney MJ. 2000. Dual roles for c-Jun N-terminal kinase in developmental and stress responses in cerebellar granule neurons. J Neurosci 20:7602–7613.

Conant K, Garzino-Demo A, Nath A, McArthur JC, Halliday W, Power C, Gallo RC, Major EO. 1998. Induction of monocyte chemoattractant protein-1 in HIV-1 Tat-stimulated astrocytes and elevation in AIDS dementia. Proc Natl Acad Sci USA 95:3117–3121.

Coughlan CM, McManus CM, Sharron M, Gao Z, Murphy D, Jaffer S, Choe W, Chen W, Hesselgesser J, Gaylord H, Kalyuzhny A, Lee VM, Wolf B, Doms RW, Kolson DL. 2000. Expression of multiple functional chemokine receptors and monocyte chemoattractant protein-1 in human neurons. Neuroscience 97:591–600.

Davis AA, Temple S. 1994. A self-renewing multipotential stem cell in embryonic rat cerebral cortex. Nature 372:263–266.

Dutt P, Wang JF, Groopman JE. 1998. Stromal cell-derived factor-1 alpha and stem cell factor/kit ligand share signaling pathways in hemopoietic progenitors: a potential mechanism for cooperative induction of chemotaxis. J Immunol 161:3652–3658.

Epstein LG, Gelbard HA. 1999. HIV-1-induced neuronal injury in the developing brain. J Leukoc Biol 65:453–457.

Erichsen D, Lopez AL, Peng H, Niemann D, Williams C, Bauer M, Morgello S, Cotter RL, Ryan LA, Ghorpade A, Gendelman HE, Zheng J. 2003. Neuronal injury regulates fractalkine: relevance for HIV-1 associated dementia. J Neuroimmunol 138:144–155.

Fallon J, Reid S, Kinyamu R, Opole I, Opole R, Baratta J, Korc M, Endo TL, Duong A, Nguyen G, Karkehabadhi M, Twardzik D, Patel S, Loughlin S. 2000. In vivo induction of massive proliferation, directed migration, and differentiation of neural cells in the adult mammalian brain. Proc Natl Acad Sci USA 97:14686–14691.

Gabuzda D, He J, Ohagen A, Vallat A. 1998. Chemokine receptors in HIV-1 infection of the central nervous system. Immunology 10:203-213.

Gage FH. 2000. Mammalian neural stem cells. Science 287:1433–1438.

Gage FH. 2002. Neurogenesis in the adult brain. J Neurosci 22:612–613.

Gendelman HE, Persidsky Y, Ghorpade A, Limoges J, Stins M, Fiala M, Morrisett R. 1997. The neuropathogenesis of the AIDS dementia complex. Aids 11(Suppl):35–45.

Glass JD, Fedor H, Wesselingh SL, McArthur JC. 1995. Immunocytochemical quantitation of human immunodeficiency virus in the brain: correlations with dementia. Ann Neurol 38:755–762.

Glass JD, Wesselingh SL, Selnes OA, McArthur JC. 1993. Clinical neuropathologic correlation in HIV-associated dementia. Neurology 43:2230–2237.

Gould E, Gross CG. 2002. Neurogenesis in adult mammals: some progress and problems. J Neurosci 22:619–623.

Gould E, Reeves AJ, Graziano MS, Gross CG. 1999. Neurogenesis in the neocortex of adult primates. Science 286:548–552.

Hazel T, Muller T. 1997. Culture of neuroepithelial stem cells. In: Crawley J, Gerfen C, McKay RDG, Rogawski M, Sibley D, Skolnick P, editors. Current protocols in neuroscience. New York: John Wiley and Sons. page 3.1.1–3.1.6.

He J, Chen Y, Farzan M, Choe H, Ohagen A, Gartner S, Busciglio J, Yang X, Hofmann W, Newman W, Mackay CR, Sodroski J, Gabuzda D. 1997. CCR3 and CCR5 are co-receptors for HIV-1 infection of microglia. Nature 385:645–649.

Hesselgesser J, Taub D, Baskar P, Greenberg M, Hoxie J, Kolson DL, Horuk R. 1998. Neuronal apoptosis induced by HIV-1 gp120 and the chemokine SDF-1alpha mediated by the chemokine receptor CXCR4. Curr Biol 8:595–598.

Jazin E, Soderstrom S, Ebendal T, Larhammar D. 1997. Embryonic expression of the mRNA for the rat homologue of the fusin/CXCR4 HIV-1 co-receptor. J Neuroimmunol 79:148–154.

Kaul M, Garden GA, Lipton SA. 2001. Pathways to neuronal injury and apoptosis in HIV-associated dementia. Nature 410:988–994.

Kaul M, Lipton SA. 1999. Chemokines and activated macrophages in HIV gp120-induced neuronal apoptosis. Proc Natl Acad Sci USA 96:8212–8216.

Kempermann G, Kuhn HG, Gage FH. 1997. More hippocampal neurons in adult mice living in an enriched environment. Nature 386:493–495.

Kintner C. 2002. Neurogenesis in embryos and in adult neural stem cells. J Neurosci 22:639–643.

Klein RS, Rubin JB, Gibson HD, DeHaan EN, Alvarez-Hernandez X, Segal RA, Luster AD. 2001. SDF-1 alpha induces chemotaxis and enhances Sonic hedgehog-induced proliferation of cerebellar granule cells. Development 128:1971–1981.

Kolson DL, Gonzalez-Scarano F. 2000. HIV and HIV dementia. J Clin Invest 106:11–13.

Langford D, Sanders VJ, Mallory M, Kaul M, Masliah E. 2002. Expression of stromal cell-derived factor 1alpha protein in HIV encephalitis. J Neuroimmunol 127:115–126.

Lataillade JJ, Clay D, Bourin P, Herodin F, Dupuy C, Jasmin C, Bousse-Kerdiles MC. 2002. Stromal cell-derived factor 1 regulates primitive hematopoiesis by suppressing apoptosis and by promoting G(0)/G(1) transition in CD34(+) cells: evidence for an autocrine/paracrine mechanism. Blood 99:1117–1129.

Lazarini F, Casanova P, Tham TN, De Clercq E, Arenzana-Seisdedos F, Baleux F, Dubois-Dalcq M. 2000. Differential signalling of the chemokine receptor CXCR4 by stromal cell- derived factor 1 and the HIV glycoprotein in rat neurons and astrocytes. Eur J Neurosci 12:117–125.

Lendahl U, Zimmerman LB, McKay RD. 1990. CNS stem cells express a new class of intermediate filament protein. Cell 60:585–595.

Lipton SA, Gendelman HE. 1995. Dementia associated with the acquired immunodeficiency syndrome. N Engl J Med 16:934–940.

Liu J, Solway K, Messing RO, Sharp FR. 1998. Increased neurogenesis in the dentate gyrus after transient global ischemia in gerbils. J Neurosci 18:7768–7778.

Lu L, Su WJ, Yue W, Ge X, Su F, Pei G, Ma L. 2001. Attenuation of morphine dependence and withdrawal in rats by venlafaxine, a serotonin and noradrenaline reuptake inhibitor. Life Sci 69:37–46.

Lu M, Grove EA, Miller RJ. 2002. Abnormal development of the hippocampal dentate gyrus in mice lacking the CXCR4 chemokine receptor. Proc Natl Acad Sci USA 99:7090–7095.

Ma Q, Jones D, Borghesani PR, Segal RA, Nagasawa T, Kishimoto T, Bronson RT, Springer TA. 1998. Impaired B -lymphopoiesis, myelopoiesis, and derailed cerebellar neuron migration in CXCR4 and SDF 1 deficient mice. Proc Natl Acad Sci USA 95:9448–9453.

Mackay CR. 2001. Chemokines: immunology's high impact factors. Nat Immunol 2:95–101.

Magavi SS, Leavitt BR, Macklis JD. 2000. Induction of neurogenesis in the neocortex of adult mice. Nature 405:951–955.

Masliah E, Heaton RK, Marcotte TD, Ellis RJ, Wiley CA, Mallory M, Achim CL, McCutchan A, Nelson JA, Atkinson JH, Grant I. 1997. Dendritic injury is a pathological substrate for human immunodeficiency virus-related cognitive disorders. Ann Neurol 42:963–972.

McArthur JC, Sacktor N, Selnes O. 1999. Human immunodeficiency virus-associated dementia. Semin Neurol 19:129–150.

McTigue D, Tani M, Krivacic K, Chernosky A, Kelner G, Maciejewski D, Maki R, Ransohoff R, Stokes B. 1998. Selective chemokine mRNA accumulation in the rat spinal cord after contusion injury. J Neurosci Res 53:368–376.

Messam CA, Hou J, Berman JW, Major EO. 2002. Analysis of the temporal expression of nestin in human fetal brain derived neuronal and glial progenitor cells. Brain Res Dev Brain Res 134:87–92.

Meucci O, Fatatis A, Simen AA, Bushell TJ, Gray PW, Miller RJ. 1998. Chemokines regulate hippocampal neuronal signaling and gp120 neurotoxicity. Proc Natl Acad Sci USA 95:14500–14505.

Meucci O, Fatatis A, Simen AA, Miller RJ. 2000. Expression of CX3CR1 chemokine receptors on neurons and their role in neuronal survival. Proc Natl Acad Sci USA 97:8075–8080.

Molyneaux KA, Zinszner H, Kunwar PS, Schaible K, Stebler J, Sunshine MJ, O'Brien W, Raz E, Littman D, Wylie C, Lehmann R. 2003. The chemokine SDF1/CXCL12 and its receptor CXCR4 regulate mouse germ cell migration and survival. Development 130:4279–4286.

Monaco MC, Sabath BF, Durham LC, Major EO. 2001. JC virus multiplication in human hematopoietic progenitor cells requires the NF-1 class D transcription factor. J Virol 75:9687–9695.

Nakatomi H, Kuriu T, Okabe S, Yamamoto S, Hatano O, Kawahara N, Tamura A, Kirino T, Nakafuku M. 2002. Regeneration of hippocampal pyramidal neurons after ischemic brain injury by recruitment of endogenous neural progenitors. Cell 110:429–441.

Nath A, Geiger J. 1998. Neurobiological aspects of human immunodeficiency virus infection: neurotoxic mechanisms. Prog Neurobiol 54:19–33.

Parent JM, Yu TW, Leibowitz RT, Geschwind DH, Sloviter RS, Lowenstein DH. 1997. Dentate granule cell neurogenesis is increased by seizures and contributes to aberrant network reorganization in the adult rat hippocampus. J Neurosci 17:3727–3738.

Ransohoff RM, Kivisakk P, Kidd G. 2003. Three or more routes for leukocyte migration into the central nervous system. Nat Rev Immunol 3:569–581.

Rossi D, Zlotnik A. 2000. The biology of chemokines and their receptors. Annu Rev Immunol 18:217–242.

Rostasy K, Egles C, Chauhan A, Kneissl M, Bahrani P, Yiannoutsos C, Hunter DD, Nath A, Hedreen JC, Navia BA. 2003. SDF-1alpha is expressed in astrocytes and neurons in the AIDS dementia complex: an in vivo and in vitro study. J Neuropathol Exp Neurol 62:617–626.

Schuldiner M, Yanuka O, Itskovitz-Eldor J, Melton DA, Benvenisty N. 2000. From the cover: effects of eight growth factors on the differentiation of cells derived from human embryonic stem cells. Proc Natl Acad Sci USA 97:11307–11312.

Shirozu M, Nakano T, Inazawa J, Tashiro K, Tada H, Shinohara T, Honjo T. 1995. Structure and chromosomal localization of the human stromal cell-derived factor 1 (SDF1) gene. Genomics 28:495–500.

Strizki JM, Albright AV, Sheng H, O'Connor M, Perrin L, Gonzalez-Scarano F. 1996. Infection of primary human microglia and monocyte-derived macrophages with human immunodeficiency virus type 1 isolates: evidence of differential tropism. J Virol 70:7654–7662.

Stumm RK, Rummel J, Junker V, Culmsee C, Pfeiffer M, Krieglstein J, Hollt V, Schulz S. 2002. A dual role for the SDF-1/CXCR4 chemokine receptor system in adult brain: isoform-selective regulation of SDF-1 expression modulates CXCR4-dependent neuronal plasticity and cerebral leukocyte recruitment after focal ischemia. J Neurosci 22:5865–5878.

Stumm RK, Zhou C, Ara T, Lazarini F, Dubois-Dalcq M, Nagasawa T, Hollt V, Schulz S. 2003. CXCR4 regulates interneuron migration in the developing neocortex. J Neurosci 23:5123–5130.

Tamamura H, Omagari A, Hiramatsu K, Gotoh K, Kanamoto T, Xu Y, Kodama E, Matsuoka M, Hattori T, Yamamoto N, Nakashima H, Otaka A, Fujii N. 2001. Development of specific CXCR4 inhibitors possessing high selectivity indexes as well as complete stability in serum based on an anti-HIV peptide T140. Bioorg Med Chem Lett 11:1897–1902.

Tamamura H, Xu Y, Hattori T, Zhang X, Arakaki R, Kanbara K, Omagari A, Otaka A, Ibuka T, Yamamoto N, Nakashima H, Fujii N. 1998. A low-molecular-weight inhibitor against the chemokine receptor CXCR4: a strong anti-HIV peptide T140. Biochem Biophys Res Commun 253:877–882.

Tong N, Perry SW, Zhang Q, James HJ, Guo H, Brooks A, Bal H, Kinnear SA, Fine S, Epstein LG, Dairaghi D, Schall TJ, Gendelman HE, Dewhurst S, Sharer LR, Gelbard HA. 2000. Neuronal fractalkine expression in HIV-1 encephalitis: roles for macrophage recruitment and neuroprotection in the central nervous system. J Immunol 164:1333–1339.

Tran PB, Miller RJ. 2003. Chemokine receptors: signposts to brain development and disease. Nat Rev Neurosci 4:444–455.

Uchida N, Buck DW, He D, Reitsma MJ, Masek M, Phan TV, Tsukamoto AS, Gage FH, Weissman IL. 2000. Direct isolation of human central nervous system stem cells. Proc Natl Acad Sci USA 97:14720–14725.

van Praag H, Kempermann G, Gage FH. 1999. Running increases cell proliferation and neurogenesis in the adult mouse dentate gyrus. Nat Neurosci 2:266–270.

Xia M, Hyman BT. 1999. Chemokines/chemokine receptors in the central nervous system and Alzheimer's disease. J Neurovirol 5:32–41.

Youn BS, Mantel C, Broxmeyer HE. 2000. Chemokines, chemokine receptors and hematopoiesis. Immunol Rev 177:150–174.

Zhang K, McQuibban GA, Silva C, Butler GS, Johnston JB, Holden J, Clark-Lewis I, Overall CM, Power C. 2003. HIV-induced metalloproteinase processing of the chemokine stromal cell derived factor-1 causes neurodegeneration. Nat Neurosci 6:1064–1071.

Zheng J, Niemann D, Bauer M, Williams C, Lopez A, Erichsen D, Ryan LA, Cotter RL, Ghorpade A, Swindells S, Gendelman HE. 2001. HIV-1 glia interactions in interleukin-8 and growth-related oncogene a secretion, neuronal signaling and demise: relevance for HIV-1-associated dementia. Conf Retroviruses Opportunistic Infect 8:227.

Zheng J, Thylin M, Ghorpade A, Xiong H, Persidsky Y, Cotter R, Niemann D, Che M, Zeng Y, Gelbard H, Shepard R, Swartz J, Gendelman H. 1999. Intracellular CXCR4 signaling, neuronal apoptosis and neuropathogenic mechanisms of HIV-1-associated dementia. J Neuroimmunol 98:185–200.

Zhu Y, Yu T, Zhang XC, Nagasawa T, Wu JY, Rao Y. 2002. Role of the chemokine SDF-1 as the meningeal attractant for embryonic cerebellar neurons. Nat Neurosci 5:719–720.

Zou YR, Kottmann AH, Kuroda M, Taniuchi I, Littman DR. 1998. Function of the chemokine receptor CXCR4 in haematopoiesis and in cerebellar development. Nature 393:595–599.

Available online at www.sciencedirect.com
SCIENCE DIRECT®
ELSEVIER
Biochemical and Biophysical Research Communications 320 (2004) 226–232
BBRC
www.elsevier.com/locate/ybbrc

A single treatment with microcapsules containing a CXCR4 antagonist suppresses pulmonary metastasis of murine melanoma

M. Takenaga,[a,*] H. Tamamura,[b] K. Hiramatsu,[b] N. Nakamura,[a] Y. Yamaguchi,[a] A. Kitagawa,[a] S. Kawai,[a] H. Nakashima,[c] N. Fujii,[b] and R. Igarashi[a]

[a] *Institute of Medical Science, St. Marianna University School of Medicine, Kawasaki 216-8512, Japan*
[b] *Graduate School of Pharmaceutical Sciences, Kyoto University, Sakyo-ku, Kyoto 606-8501, Japan*
[c] *Department of Microbiology, St. Marianna University School of Medicine, Kawasaki 216-8511, Japan*

Received 15 May 2004
Available online 10 June 2004

Abstract

Biodegradable poly D,L-lactic acid (PLA, molecular weight: ca. 5000) microcapsules containing a CXCR4 antagonist (4F-benzoyl-TE14011) were prepared (4F-benzoyl-TE14011-PLA), and their anti-metastatic activity was evaluated in mice. A single subcutaneous administration of 4F-benzoyl-TE14011-PLA significantly reduced the number of colonies formed by pulmonary metastasis of B16–BL6 melanoma cells expressing CXCR4. The same dose of 4F-benzoyl-TE14011 in a single or a series of treatments affected little. The substance 4F-benzoyl-TE14011 dose-dependently suppressed B16–BL6 cell growth. In the cells cultured with SDF-1, a more potent suppression was observed. 4F-Benzoyl-TE14011 was rapidly released from 4F-benzoyl-TE14011-PLA for an initial period, both in vitro and in vivo. A steady release was thereafter observed. Therefore, this drug release profile might contribute to prevention of melanoma metastasis at the steps involving the migration and cell growth. These results also show that a sustained drug release formulation could be a useful drug delivery system for CXCR4 antagonists.

Keywords: B16–BL6; CXCR4 antagonist; Melanoma; Metastasis; Poly D,L-lactic acids; Sustained release

CXCR4 is a member of the GPCR protein family and is the receptor for a chemokine, stromal cell-derived factor (SDF)-1 [1,2]. The interaction with SDF-1 induces chemotaxis, immunomodulation, and other regulatory functions. CXCR4 also plays an important role in human immunodeficiency virus type-1 (HIV-1) infection. An HIV-1 envelope glycoprotein, gp120, initially binds to a CD4 molecule on the host cell surface [3]. This interaction leads to conformational changes in gp120 that increases its affinity for the HIV-1 co-receptor, the chemokine receptor CXCR4 or CCR5 [4,5]. Subsequent association of gp120 with CXCR4 or CCR5 promotes conformational changes in an HIV-1 transmembrane envelope glycoprotein, gp41 [6], leading to membrane fusion. The binding of HIV to CXCR4 is therefore of paramount importance to the viral infection.

Recently, CXCR4 has been reported to be involved in cancer metastasis [7–12]. Cancer metastasis is a complex event with many factors and steps. Robledo et al. [9] reported that human melanoma cells express the chemokine receptors CXCR3 and CXCR4, which mediate agonist-dependent cell migration and activation, and that these receptors might be relevant to tumor cell invasion and growth. Müller et al. [7] demonstrated that primary tumors of breast cancer and melanoma cell lines express CXCR4 as well as CCR7 at the messenger RNA level. Moreover, exposure of breast cancer cells to a function-blocking anti-CXCR4 mAb inhibited metastasis to the lungs, suggesting that CXCR4 might be involved in the selective metastasis of cancer cells. Furthermore, based on in vitro adhesion and chemotaxis experiments, several investigators have suggested roles for SDF-1 and CXCR4 in the metastasis of

* Corresponding author. Fax: +81-44-976-3747.
E-mail address: m2take@marianna-u.ac.jp (M. Takenaga).

0006-291X/$ - see front matter © 2004 Elsevier Inc. All rights reserved.
doi:10.1016/j.bbrc.2004.05.155

neuroblastoma [8], melanoma [9], and prostate cancer cells [10]. Murakami et al. [13] showed that an excessive expression of CXCR4 dramatically enhanced the metastatic accumulation of B16 melanoma cells in mice lungs. They also showed that the CXCR4 antagonist T22, developed in our laboratory [14], blocked pulmonary metastasis in mice injected with B16 cells transduced with CXCR4.

The T22 analog 4F-benzoyl-TE14011 used in the present study is one of the most potent CXCR4 antagonists that we have synthesized [14–20]. Its EC_{50} value, evaluated as anti-HIV activity in HIV-1-infected MT-4 cells, was 2.4 nM. However, due to its hydrophilicity and small molecular size, it might be rapidly eliminated from the body after dosing.

We have recently investigated a sustained-release formulation of insulin, for therapy of diabetic patients who require multiple dosages. We have developed this formulation by encapsulating insulin with a biodegradable polymer, poly co-poly(D,L-lactic/glycolic) acid (PLGA) [21–23]. Formulations prepared using biodegradable polymers such as PLGA and PLA have attractive attributes for a controlled and sustained release of drugs. In contrast to insulin, 4F-benzoyl-TE14011 would not require a strict controlled release. Since a single treatment can be effective for a long period, the formulation would be a valuable development, not only for anti-cancer-metastatic agents but also anti-HIV agents. The present study focused on the possibility of developing a sustained release formulation of 4F-benzoyl-TE14011.

Materials and methods

Reagents. 4F-Benzoyl-TE14011 was synthesized as reported previously [20]. Anti-human CXCR4-phycoerythrin (clone 12G5) was purchased from R&D systems (Minneapolis, MN). SDF-1 was purchased from ProTech EC (London, UK).

Cells. B16–BL6 mouse melanoma cells were maintained in Dulbecco's modified Eagle's medium (Sigma Chemical, MO) supplemented with 10% heat-inactivated fetal bovine serum (FBS, Sanko Junyaku, Tokyo, Japan) and 100 U/ml penicillin and 100 μg/ml streptomycin (Gibco, Grand Island, NY).

Animals. Six-week-old male C57BL/6 or ICR mice were purchased from SLC Experimental Animals (Shizuoka, Japan). Animals were housed at a constant temperature (23 ± 1 °C) and humidity (50–60%) with free access to a standard diet and water. The animal room had a 12-h light/dark cycle (lights on from 6:30 to 18:30). The study protocol was approved by the Animal Experimentation Committee of St. Marianna University.

PLA microcapsules containing a CXCR4 antagonist. The preparation method was based on the double emulsion diffusion technique. 4F-Benzoyl-TE14011 (50 mg) and fatty acid ester saccharide (50 mg, J-1216, Mitsubishi-Kagaku Food Corporation, Tokyo, Japan) were dissolved in 2 ml of distilled water. This solution was poured into 20 ml of an acetone/methylene chloride (1:1, v/v) solution containing PLA (450 mg) and fatty acid ester saccharide (50 mg, J-1205, Mitsubishi-Kagaku Food Corporation). A water-in-oil (w/o) emulsion was then formed by stirring at 4000 rpm. This w/o emulsion was further added to a 0.5% carboxymethylcellulose (CMC) aqueous solution with stirring to achieve the (water-in-oil)-in-water (w/o/w) double emulsion system. This emulsion was stirred at 1200 rpm for 24 h to reduce the organic solvent volume. Lyophilization then gave the formulated drug (4F-benzoyl-TE14011-PLA). Particle size was determined by using a particle analyzer (Multisizer IIE, Beckman Coulter, Tokyo, Japan). The CXCR4 antagonist-loaded microcapsules were examined under a SEM 4300 scanning electron microscope (Hitachi, Ibaraki, Japan) at an acceleration voltage of 1.0 kV. The 4F-benzoyl-TE14011 contents of the prepared microcapsules were determined after extraction with methylene chloride and 0.01 M HCl according to the method of Lowry et al. [24], using 4F-benzoyl-TE14011 as a standard.

Experimental pulmonary metastasis of B16–BL6 melanoma cells. Anti-melanoma-metastatic activity was assessed using an experimental metastasis assay. Mice were inoculated via the tail vein with 1×10^4 viable B16–BL6 cells and were sacrificed by decapitation 2 weeks after tumor inoculation. The lungs were isolated, fixed with 70 (v/v)% ethanol, and examined for tumor nodules. The number of metastatic nodules on the lungs was counted in each mouse under a dissecting microscope. Drugs were administered subcutaneously 30 min before tumor cell inoculation. Daily treatment with 4F-benzoyl-TE14011 was carried out at approximately 10 o'clock in the morning. 4F-Benzoyl-TE14011-PLA was dispersed (10 w/v%) with 5% mannitol solution at pH 6.5 containing 0.5% CMC and 0.1% Tween 80, just before administration. An Alzet osmotic pump (duration, 14 days, pumping rate, 0.25 μl/h, Model 1002, ALZA, Mountain View, CA, USA) containing 35.7 mg/ml of 4F-benzoyl-TE14011 (100 μl in saline) was implanted subcutaneously 30 min before tumor cell transplantation.

Anti-HIV activity of mouse sera following the subcutaneous injection of the formulation. Male ICR mice were treated by a single injection of 4F-benzoyl-TE14011-PLA using a subcutaneous route. Blood samples were obtained from the inferior ophthalmic vein before and after this treatment.

The anti-HIV activity of serum samples on 2.5×10^4 Molt-4 cells infected with HIV-1 (HIV-1 IIIB, activity: 52×10^4 $TCID_{50}$/ml) was assessed by MTT assay as previously described [25].

In vitro release. 4F-Benzoyl-TE14011-PLA (100 mg) was suspended in 1.0 ml of phosphate-buffered saline (PBS) (pH 7.4) in a test tube and kept at 37 °C. At appropriate intervals, supernatants were collected after centrifugation, 1.0 ml of the buffer was added, and the mixture was further incubated. The content of the supernatant was determined by the method of Lowry et al. [24] using 4F-benzoyl-TE14011 as a standard.

Immunohistochemistry. B16–BL6 cells were fixed with 4% paraformaldehyde in PBS (pH 7.4) for 24 h and washed by PBS, followed by treatment with 0.5% Triton-X in PBS for 5 min.

Mice were anesthetized and perfused with 4% paraformaldehyde in PBS by intracardiac injection. Lungs were fixed by immersion in fresh fixative for 1 h at room temperature. Tissue was cryoprotected by immersion in 10% sucrose in PBS for 1 h at room temperature and overnight in 30% sucrose in PBS at 4 °C. After cryoprotection, lungs were frozen in embedding OTC compound (Tissue Tek, Sakura, Torrance, CA), and then cut into 5 μm sections on a cryostat and placed on poly-L-lysine-coated glass slides.

After fixation and blocking by 5% BSA in PBS, lung sections were reacted overnight with phycoerythrin-conjugated anti-CXCR4 antibody. Fluorescence images were acquired using a conventional microscope equipped with epifluorescence optics (model IX71/CoolSNAP-HQ, Olympus, Melville, NY). Hematoxylin–eosin staining was also carried out.

Cell growth. B16–BL6 cells (1×10^3) suspended in FCS-free culture medium were seeded into a 96-well tissue culture plate. 4F-Benzoyl-TE14011 was dissolved in PBS (pH 7.4) and diluted by DMEM to make the desired concentrations. Various concentrations of 4F-benzoyl-TE14011 were cultured with cells for 3 days in a humidified atmosphere of 5% CO_2 in air at 37 °C. Cell growth was assessed by [^{3}H]thymidine (methyl[1′,2′-^{3}H]thymidine (1.40 TBq/mmol),

Amersham, UK) incorporation over the last 4 h of incubation. The radioactivity was counted with a scintillation counter (MicroBeta TRILUX, Pharmacia, Sweden). Cell growth was also examined in the presence of SDF-1.

Statistical analysis. Statistical analysis was performed by using Mann–Whitney U test and $p < 0.05$ was taken as indicating significance.

Results

PLA microcapsules containing 4F-benzoyl-TE14011

Morphological examination study using a scanning electron microphotograph showed spherical surfaces of the PLA particles, with a diameter of 14.57 ± 11.21 μm. The 4F-benzoyl-TE14011 content was 5.6%, indicating that the loading efficacy was approximately 90%.

Experimental pulmonary metastasis of B16–BL6 melanoma cells in mice

In the vehicle-treated control group, the number of pulmonary metastatic nodules was 196.4 ± 58.6 (mean ± SE) per mouse (Fig. 1). 4F-Benzoyl-TE14011-PLA reduced the number of colony formations, even though not preventing metastatic incidence. When 4F-benzoyl-TE14011-PLA (3 mg as 4F-benzoyl-TE14011) was injected to mice, the number of metastatic nodules was 122.9 ± 42.6 per mouse, which was significantly lower than that in the control group ($p < 0.05$). The PLA formulation alone showed no effect (192.3 ± 56.1). Bolus subcutaneous injection of the parent agent, 4F-benzoyl-TE14011 (3 mg), showed no significant difference compared with the control group. Daily treatment by subcutaneous injection of 4F-benzoyl-TE14011 (300 μg/mouse) for 10 days showed a partial, but not significant, reduction (178.9 ± 65.8). Subcutaneous injection of 4F-benzoyl-TE14011 using an Alzet pump implanted before tumor cell inoculation also reduced the number of colony formations (162.5 ± 47.9).

When 4F-benzoyl-TE14011-PLA was treated 30 min after tumor cell inoculation, the number of metastatic nodules was also reduced. However, there was no significant difference. (168 ± 42.5, vs. control 201.4 ± 49.1). On day 14, the formulation of 4F-benzoyl-TE14011-PLA was detected little at the injected site. The 4F-benzoyl-TE14011-treated group showed a tendency to reduce the metastatic nodule overall size, but not significance.

Anti-HIV activity of mouse sera following the subcutaneous administration of the formulation

The anti-HIV activity of serum samples is thought to reflect the plasma concentrations of 4F-benzoyl-TE14011 after subcutaneous injection of 4F-benzoyl-TE14011-PLA. 4F-Benzoyl-TE14011-PLA (3 mg as 4F-benzoyl-TE14011) showed a transient augmentation of anti-HIV activity (Fig. 2A). Thereafter, the activity again increased and then gradually decreased. A single injection of 4F-benzoyl-TE14011 showed only a transient increase of anti-HIV activity.

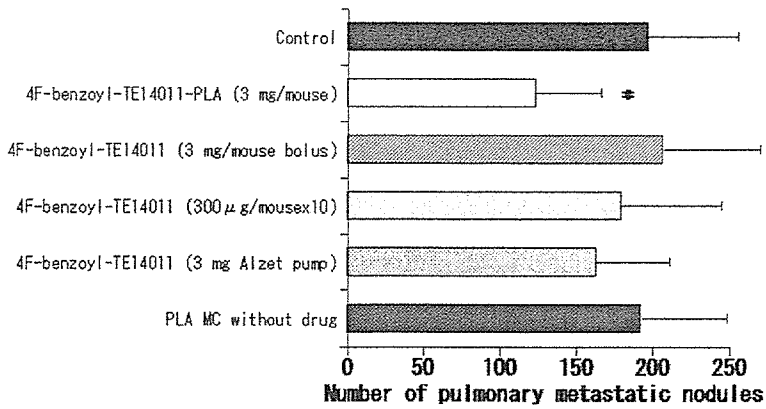

4F-benzoyl-Arg-Arg-Nal-Cys-Tyr-Cit-Lys-D-Glu-Pro-Tyr-Arg-Cit-Cys-Arg-NH$_2$

Nal = L-3-(2-naphthyl)alanine, Cit = L-citrulline

Fig. 1. Effects of 4F-benzoyl-TE14011-PLA on experimental pulmonary metastasis. B16–BL6 cells (1×10^4/0.2 ml) were injected into the tail veins of mice. 4F-Benzoyl-TE14011-PLA, 4F-benzoyl-TE14011 (bolus injection, 3 mg drug), 4F-benzoyl-TE14011 (300 μg/mouse/day for 10 days), 4F-benzoyl-TE14011 (Alzet pump, constant release of total 3 mg 4F-benzoyl-TE14011 over 2 weeks), or PLA microcapsules (MC) without drug was administered through a subcutaneous route 30 min prior to tumor cell inoculation. Alzet pump containing 4F-benzoyl-TE14011 was also implanted 30 min before tumor cell injection. On day 14, mice were sacrificed, and tumor nodules on the surface of the lungs were counted. The chemical structure of 4F-benzoyl-TE14011 was shown below. Data represent means ± SE. $n = 5$–8. *$p < 0.05$, vs. control.

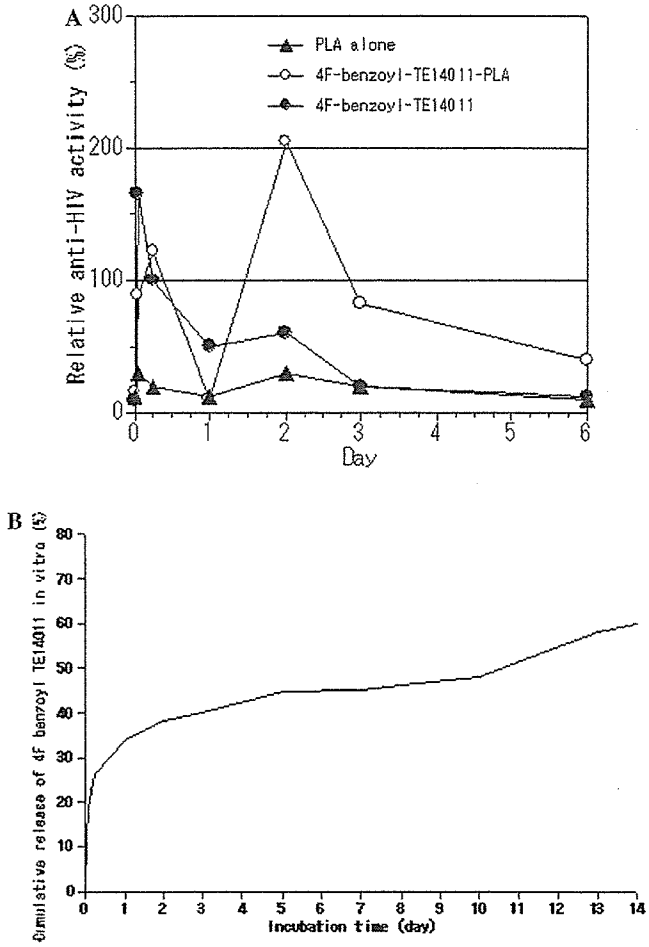

Fig. 2. (A) Serum anti-HIV activity following subcutaneous treatment of 4F-benzoyl-TE14011-PLA and (B) In vitro drug release from 4F-benzoyl-TE14011-PLA. (A) Serum anti-HIV activity following subcutaneous treatment of 4F-benzoyl-TE14011-PLA (3 mg as 4F-benzoyl-TE14011), 4F-benzoyl-TE14011 (bolus injection, 3 mg drug), or PLA alone was determined as described in Materials and methods. The relative anti-HIV activity was calculated from the concentration required for ED80. Data are means obtained from 3 mice. (B) In vitro 4F-benzoyl-TE14011 release from 4F-benzoyl-TE14011-PLA was evaluated. Data represent means obtained from 3 to 5 separate experiments.

In vitro release of 4F-benzoyl-TE14011 from 4F-benzoyl-TE14011-PLA

The in vitro release from 4F-benzoyl-TE14011-PLA was examined (Fig. 2B). The cumulative amount of 4F-benzoyl-TE14011 released from 4F-benzoyl-TE14011-PLA was 11.7% (2 h) and 33.8% (1 day). An acceleration of drug release was again seen after 10 days incubation.

Expression of CXCR4 on B16–BL6 cells and lung specimen

Immuno-fluorescence microscopic analysis demonstrated that B16–BL6 cells express CXCR4 on their surface (Figs. 3A and B). CXCR4 expression in the lung sections was also observed, especially along the epithelial cells Figs. 3C and D.

Cell growth and CXCR4 expression of lung specimens after B16–BL6 melanoma inoculation

HE staining revealed that tumor cells migrated and grew around not only the epithelial cells but also blood vessels (Fig. 3F). They also grew on the surface of lung (Figs. 3G and H). The metastatic nodule on the surface of lung showed CXCR4 expression 2 weeks after cell inoculation (Figs. 3I and J). Lung sections of mice (Figs. 3H and I) were ones treated with 4F-benzoyl-TE14011-PLA, and the sections (Figs. 3F, G, and J) were control. The intensity of the CXCR4 expression following nodule formation showed no significant difference between the two. However, the grown tumor cells were localized less around the epithelial cells in the 4F-benzoyl-TE14011-PLA-treated group.

Effect of 4F-benzoyl-TE14011 on cell growth

The growth of B16–BL6 cells was examined under conditions that included extremely low concentrations of serum. Dose-dependent suppression of the cell growth was observed by the treatment with 4F-benzoyl-TE14011 (Table 1). 4F-Benzoyl-TE14011 (300 μg/ml) reduced thymidine incorporation (dpm) by one-tenth. The inhibitory activity was less under serum conditions (data not shown).

SDF-1 enhanced the cell growth by nearly 2-fold compared to that in the absence of SDF-1. It should be noted that even 3 μg/ml of 4F-benzoyl-TE14011 significantly reduced the cell growth.

Discussion

Our present study showed that a subcutaneous single administration of 4F-benzoyl-TE14011-PLA, a biodegradable polymer microcapsule formulation containing a CXCR4 antagonist (4F-benzoyl-TE14011), significantly reduced the number of colonies formed by pulmonary metastasis of B16–BL6 melanoma cells.

CXCR4 antagonists have been identified as anti-HIV agents [26–29]. 4F-Benzoyl-TE14011 is one of the most potent CXCR4 antagonists that we have synthesized based on T22 and its smaller analog, T140 [14–20]. 4F-Benzoyl-TE14011, more potent than AZT in the MTT assay, is stable in mouse serum and rat liver homogenate [20].

4F-Benzoyl-TE14011-PLA was proven to have anti-melanoma metastatic activity following a single subcutaneous dosing, indicating that this drug delivery system is promising. Murakami et al. [13] have already shown

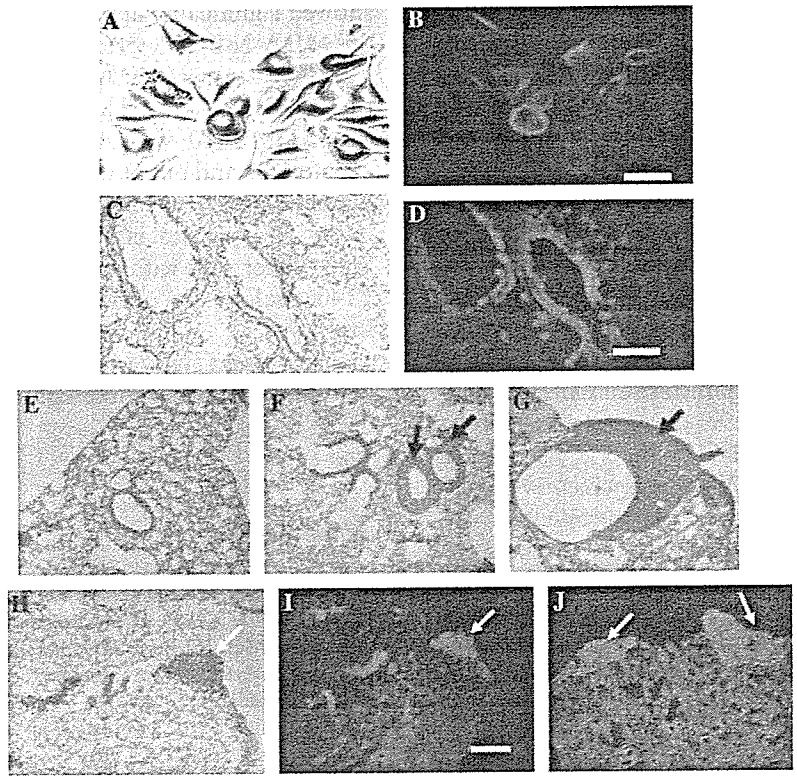

Fig. 3. B16–BL6 melanoma cells and lung specimen before or after cell inoculation. (A,B) B16–BL6 melanoma cells (scale bar is 10 μm.) (C–E) The normal lung section (scale bar is 20 μm.) (F–J) The lung section 2 weeks after tumor cell inoculation. Arrow; tumor cell growth. (B, D, I, and J) Immunostaining of CXCR4 was performed. (E–H) Hematoxylin–eosin (HE) staining.

Table 1
Effects of 4F-benzoyl-TE14011 on the SDF-1-stimulated cell growth in vitro

Addition of SDF-1 (ng/ml)	4F-benzoyl-TE14011 (μg/ml)				
	0	0.3	3	30	300
0	6698.1 ± 1962.9	8115.7 ± 1733.0	7556.0 ± 1892.0	6187. ± 1444.2	530.3 ± 516.5**
5	11128.9 ± 1417.0#	9320.5 ± 478.0	8555.1 ± 762.2*	7784.4 ± 2445.4*	845.7 ± 562.4**
50	11251.2 ± 678.7#	9622.1 ± 949.0	8916.1 ± 625.7**	7342.4 ± 573.0**	606.4 ± 224.2**

B16–BL6 cells (1×10^3/well) suspended in FCS-free culture medium were seeded to a culture plate in the presence or absence of SDF-1. Various concentrations of TE14011 were added and subsequently culture was done for 3 days. Cell growth was assessed by [^{3}H]thymidine incorporation over the last 4 h of incubation. Data are means ± SD (dpm) ($n = 8$).

#$p < 0.01$ vs. no addition of SDF-1.

*$p < 0.05$, **$p < 0.01$ vs. no addition of 4F-benzoyl-TE14011.

that daily treatment with T22 (4 μg peptide/mouse) via an i.p. route for 14 days reduced the number of nodules formed by pulmonary metastasis of melanoma cells. Even though a single treatment, 4F-benzoyl-TE14011-PLA required higher amounts of drug. This may be partly explained by the difference in the administration route. Another major reason would derive from the dependency of metastasis on the CXCR4–SDF-1 system. They demonstrated that transfection of the CXCR4 gene in B16–F10 cells dramatically enhanced the metastatic accumulation of tumor cells in the lungs of mice. B16–BL6 melanoma cell lines used in our study have a high metastatic potency, especially to the lungs. Although we confirmed the expression of CXCR4 on the surface, the metastatic potency seemed to be less dependent on the CXCR4-ligand system than that of CXCR4 gene-transfected B16–F10 cells used by Murakami et al. Therefore, their metastatic system might have required less amount of 4F-benzoyl-TE14011.

Nevertheless, it is evident that the CXCR4–SDF-1 system is involved in the growth of B16–BL6 cells. SDF-1 significantly promoted the cell growth. It was notable that the SDF-1-mediated cell growth was effectively suppressed by 4F-benzoyl-TE14011. This shows the possibility that 4F-benzoyl-TE14011 released from 4F-benzoyl-TE14011-PLA suppressed the cell growth at the metastatic destination sites in vivo. HE staining revealed that the cell growth spread not only on the surface of lungs but also around blood vessels and the epithelial cells. The grown tumor cells were associated with

CXCR4 expression. The expression was not diminished by 4F-benzoyl-TE14011-PLA, but the tumor growth was less around the epithelial cells. These evidences are support for 4F-benzoyl-TE14011 suppression of the metastatic process through CXCR4 containing cell growth.

The same dose of 4F-benzoyl-TE14011 alone (bolus injection) did not significantly reduce the number of metastatic nodules. Successive subcutaneous treatments had been expected to be potent, but no significant difference was observed. These could be partly ascribed to its easy elimination from the body, as seen in serum anti-HIV activity. Alzet pump administration causes a constant drug release without an initial large release, but it was less effective. 4F-Benzoyl-TE14011-PLA showed a transient increase of anti-HIV activity, which is consistent with an initially rapid drug release in vitro. 4F-Benzoyl-TE14011-PLA thereafter kept on releasing the drug with a lower but a relatively steady rate in vitro. This finding prompted us to advance the hypothesis that the desired pharmacological activity requires a profile with an initial large release followed by lower constant release. In vitro release study showed an acceleration of the drug release after 10 days incubation. This phenomenon was also seen in the case of insulin [21]. Plasma insulin level showed a lag phase and gradual augmentation in vivo, which was similar as in vitro release. In general, the drug release is associated with PLA polymer degradation. The serum anti-HIV activity may not completely reflect drug bio-distribution, but it might have been transiently but again higher after day 6, and have contributed to the pharmacological effect.

An advantage of formulations based on biodegradable polymers such as PLGA and PLA is an ability to maintain a relatively sustained drug release. Since these polymers are degraded by hydrolysis, followed by a drug release when exposed to aqueous media, they have been used to achieve sustained releases of various drugs [30–33]. Leuprolein acetate-loaded PLGA has already been used in a clinical setting and has made an important contribution to the remarkable improvement in the physiological condition of patients with prostate cancer, etc. A small molecular and hydrophilic drug is difficult to encapsulate, and susceptible to being released rapidly into aqueous media. PLA has an adequate entrapping efficacy for such drugs, compared to PLGA. However, PLA brings a rapid release, and there are many problems that need to be solved for achievement of a more constant release. In the present study using this system, the first rapid release of 4F-benzoyl-TE14011 might contribute to the suppression of metastasis.

4F-benzoyl-TE14011 might suppress both the migration of B16–BL6 cells into the target organs and the formation of nodules. In addition, several other papers have shown the efficacy of CXCR4 antagonists derived from T140 as anti-cancer agents: 4F-benzoyl-TN14003 showed significant suppression of pulmonary metastasis of MDA-MB-231 breast cancer cells in mice [34]. TN14003 was proven to inhibit SDF-1-induced migration and invasion of several human pancreatic cancer cells [35]. T140 was shown to block SDF-1-induced chemotaxis and attenuated the migration of pre-B acute lymphoblastic leukemia cells into bone marrow stromal layers [36], and to inhibit the interaction of small cell lung cancer cells with stromal cells [37]. Taken together, T140 analogs are promising agents for cancer chemotherapy.

The present study provides insight into the possibility of a new administration strategy for CXCR4 antagonists.

Acknowledgments

We are very grateful to Ms. Akemi Hamaguchi and Ms. Kayo Matsumoto for their excellent assistance. The authors wish to thank Prof. Scott McN. Sieburth, Department of Chemistry, Temple University, PA, USA, for proofreading the manuscript and providing useful comments.

References

[1] C.C. Bleul, M. Farzan, H. Choe, C. Parolin, I. Clark-Lewis, J. Sodroski, T.A. Springer, The lymphocyte chemoattractant SDF-1 is a ligand for LESTR/fusin and blocks HIV-1 entry, Nature 382 (1996) 829–833.

[2] E. Oberlin, A. Amara, F. Bachelerie, C. Bessaia, J.L. Virelizier, F. Arenzana-Seisdedos, O. Schwartz, J.M. Heard, I. Clark-Lewis, D.F. Legler, M. Loetscher, M. Baggiolini, B. Moser, The CXC chemokine SDF-1 is the ligand for LESTR/fusin and prevents infection by T-cell-line-adapted HIV-1, Nature 382 (1996) 833–835.

[3] A.G. Dalgleish, P.C. Beverley, P.R. Clapham, D.H. Crawford, M.F. Greaves, R.A. Weiss, The CD4 (T4) antigen is an essential component of the receptor for the AIDS retrovirus, Nature 312 (1984) 763–767.

[4] L. Wu, N.P. Gerard, R. Wyatt, H. Choe, C. Parolin, N. Ruffing, A. Borsetti, A.A. Cardoso, E. Desjardin, W. Newman, C. Gerard, J. Sodroski, CD4-induced interaction of primary HIV-1 gp120 glycoproteins with the chemokine receptor CCR-5, Nature 384 (1996) 179–183.

[5] A. Trkola, T. Dragic, J. Arthos, J.M. Binley, W.C. Olson, G.P. Allaway, C. Cheng-Mayer, J. Robinson, P.J. Maddon, J.P. Moore, CD4-dependent, antibody-sensitive interactions between HIV-1 and its co-receptor CCR-5, Nature 384 (1996) 184–187.

[6] P.L. Jones, T. Korte, R. Blumenthal, Conformational changes in cell surface HIV-1 envelope glycoproteins are triggered by cooperation between cell surface CD4 and co-receptors, J. Biol. Chem. 273 (1998) 404–409.

[7] A. Müller, B. Homey, H. Soto, N. Ge, D. Catron, M.E. Buchanan, T. McClanahan, E. Murphy, W. Yuan, S.N. Wagner, J.L. Barrera, A. Mohar, E. Verastegui, A. Zlotnik, Involvement of chemokine receptors in breast cancer metastasis, Nature 410 (2001) 50–56.

[8] H. Germinder, O. Sagi-Assif, L. Goldberg, T. Meshel, G. Rechavi, I.P. Witz, A. Ben-Baruch, A possible role for CXCR4 and its ligand, the CXC chemokine stromal cell-derived factor-1, in the